CELL BIOLOGY

USP8 and Hsp70 regulate endoreplication by synergistically promoting Fzr deubiquitination and stabilization

Wenliang Qian[1,2]*†, Xing Zhang[1,2]†, Dongqin Yuan[1,2]†, Yuting Wu[1,2], Hao Li[1,2], Ling Wei[3], Zheng Li[1,2], Zongcai Dai[1,2], Pei Song[1,2], Qiaoling Sun[1,2], Zizhang Zhou[4], Qingyou Xia[1,2], Daojun Cheng[1,2]*

Endoreplication is characterized by multiple rounds of DNA replication without cell division and determines the growth and final size of endoreplicating cells and tissues in eukaryotes. The cyclic ubiquitination and degradation of several cell cycle regulators are required for endoreplication progression. However, the deubiquitinase that deubiquitinates and stabilizes key factors to modulate endoreplication remains unknown. Here, we found in the endoreplicating *Drosophila* salivary gland and *Bombyx* silk gland that the depletion of ubiquitin-specific peptidase 8 (USP8) led to endoreplication arrest and a decrease in gland size. Mechanistically, we showed that USP8 interacted with the Fizzy-related (Fzr) protein, a conserved master regulator of endoreplication, thereby deubiquitinating and stabilizing Fzr to modulate endoreplication. Moreover, the molecular chaperone heat shock protein 70 (Hsp70) mediated proper folding of Fzr and increased the interaction between Fzr and USP8, thereby promoting the deubiquitination and stabilization of Fzr. Together, our study demonstrates that USP8 and Hsp70 regulate endoreplication by synergistically maintaining Fzr stability though deubiquitination.

INTRODUCTION

Endoreplication (also called endocycle) is a common cell cycle variant that frequently occurs in the cells of various tissues at specific developmental stages in animals and plants, which only comprises of DNA synthesis (S) and Gap (G) phases (*1*–*5*). Unlike mitotic cells, endoreplicating cells undergo multiple rounds of DNA replication but lack mitotic events, such as chromosome segregation and cytokinesis, resulting in polyploidy (*2*). Therefore, endoreplication is an effective strategy for promoting cell growth and is closely correlated with final size and physiological functions of endoreplicating tissues (*2*). In insects, endoreplication has been extensively studied in several tissues, including the salivary gland, prothoracic gland, trachea of *Drosophila* larvae, the silk gland of *Bombyx* larvae, the adult *Drosophila* ovary, and the fat body of adult female *Locusta* (*1*, *2*, *5*, *6*). The disruption of endoreplication progression substantially impedes tissue growth and impairs the production of major functional molecules, such as silk production–related silk proteins in *Bombyx* silk glands (*7*), pupa attachment–related glue proteins in *Drosophila* salivary glands (*8*), development-related ecdysteroid in *Drosophila* prothoracic glands (*9*, *10*), and oogenesis-related vitellogenin in *Locusta* fat bodies (*11*).

Fizzy-related protein (Fzr, also known as Cdh1 in mammals), a scaffold protein containing several WD40 domains that mediate protein-protein interaction (*12*, *13*), functions as a master regulator of endoreplication entry and maintenance in animals and plants (*14*–*20*). Fzr expression is up-regulated at the time of the mitosis-to-endoreplication transition during the embryonic period (*14*, *15*); the loss of Fzr function in endoreplicating cells blocks endoreplication (*7*, *10*, *14*–*17*), whereas increased Fzr expression in mitotic cells triggers endoreplication and results in enlarged cells (*14*, *21*, *22*). Mechanistically, accumulating evidence from the endoreplicating *Drosophila* salivary gland has shown that Fzr acts to activate the anaphase-promoting complex/cyclosome (APC/C) with the E3 ubiquitin ligase activity, and the APC/C^{Fzr} activity exhibits a periodic oscillation that is driven by the S phase cyclin E and cyclin-dependent kinase 2 (CycE-Cdk2) complex (*1*, *2*, *23*–*25*). In late G phase, an accumulation of transcription factor E2F1 promotes *CycE* transcription; a subsequent raise in the CycE-Cdk2 activity inhibits the activity of APC/C^{Fzr} and drives S phase initiation. During S phase, activated E3 ubiquitin ligase $CRL4^{Cdt2}$ degrades E2F1; a consequent drop in the CycE-Cdk2 activity reestablishes a G phase and also allows high activity of APC/C^{Fzr}, which then degrades geminin as an inhibitor of the prereplication complex (PreRC) and facilitates PreRC assembly for the next cycle. Thus, the ubiquitination-dependent cyclic degradation of cell cycle regulators is indispensable for the oscillation of endoreplication. In addition, previous studies in mitotic cells in *Drosophila* reveal that APC/C^{Fzr} is also required for the degradation and removal of mitotic cyclins during G_1 phase (*15*, *26*, *27*). Notably, in cultured mouse fibroblast cells, Cdh1 as a mammalian homolog of Fzr has been shown to mediate its own degradation by activating APC/C during G_1 phase (*28*). However, how the stability of Fzr/Cdh1 and other cell cycle regulators is maintained during endoreplication remains unknown.

Deubiquitination counteracts the ubiquitination process to modulate various cellular processes in cells by removing ubiquitin chains at ubiquitin-conjugated proteins and increasing protein stability (*29*–*34*). Protein deubiquitination is generally catalyzed by ubiquitin-specific proteases (USPs) of the deubiquitinase family (*29*–*33*). In *Drosophila*, 16 USPs have been discovered (*35*), and several USPs have been shown to target different substrate proteins involved in

[1]Integrative Science Center of Germplasm Creation in Western China (CHONGQING) Science City, Biological Science Research Center, Southwest University, Chongqing 400715, China. [2]State Key Laboratory of Resource Insects, Southwest University, Chongqing 400715, China. [3]School of Life Sciences, Southwest University, Chongqing 400715, China. [4]College of Life Sciences, Shandong Agricultural University, Tai'an 271018, China.
*Corresponding author. Email: chengdj@swu.edu.cn (D.C.); qianwl@swu.edu.cn (W.Q.)
†These authors contributed equally to this work.

oogenesis, wing development, aging, antiviral activity, apoptosis, and the circadian rhythm. For example, USP8 deubiquitinates and stabilizes endosomal sorting complexes required for transport-III (ESCRT-III) in ovarian germline cells and CLOCK in pacemaker neurons to orchestrate incomplete cell division and locomotor activity rhythms, respectively (*36*, *37*). USP7 targets Yorkie in the Hippo pathway or Ci in the Hedgehog pathway to modulate wing development (*38*, *39*). However, to date, whether USP-mediated deubiquitination is involved in endoreplication has never been illustrated.

In the present study, we identified USP8 as a deubiquitinase for Fzr during endoreplication in the *Drosophila* salivary gland and *Bombyx* silk gland. USP8 depletion in these two types of glands hampers endoreplication and decreases gland size. Mechanistically, USP8 interacts with Fzr to deubiquitinate and stabilize Fzr. The molecular chaperone Hsp70 promotes the interaction of Fzr with USP8 by mediating Fzr folding, thereby participating in endoreplication progression. Our work reveals a conserved mechanism by which USP8 and Hsp70 regulate endoreplication progression by synergistically maintaining Fzr stability through deubiquitination.

RESULTS

USP8 regulates endoreplication in the salivary gland and silk gland

To identify the deubiquitinases that are involved in regulating endoreplication progression and organ size in insects, we first used the *Sg*-Gal4 driver, which is specifically expressed in the endoreplicating salivary gland in *Drosophila* (*40*, *41*), to perform a salivary gland–specific RNA interference (RNAi) screening of 16 deubiquitinases, which were previously predicted from the *Drosophila* genome (*35*). We found that salivary gland–specific knockdown of only *USP8*, but not other deubiquitinases, substantially decreased the size of the salivary gland (Fig. 1A and figs. S1, A and B, and S3A) but had no effect on body size or developmental progression of *Drosophila* larvae (fig. S2). In addition, we further analyzed the effect of salivary gland–specific overexpression of a dominant-negative form of *USP8* (*USP8*^{C572A}), which is catalytically inactive but retains substrate binding capacity (*36*, *37*). Similarly, *USP8*^{C572A} overexpression in the salivary gland also decreased gland size (Fig. 1B) but did not affect larval growth or developmental progression (fig. S3, B to D).

We next examined the effect of *USP8* knockdown on endoreplication progression in the salivary gland. We observed that salivary gland–specific knockdown of *USP8*, not other deubiquitinases, decreased the *C* value and DNA content in salivary gland cells (Fig. 1, C and D, and fig. S1, C to E). An 5-ethynyl-2'-deoxyuridine (EdU) incorporation assay further revealed that DNA replication in salivary gland cells was abrogated by *USP8* knockdown (Fig. 1E). Consistently, salivary gland–specific overexpression of dominant-negative *USP8*^{C572A} also resulted in a decrease in both the *C* value and DNA content and blocked DNA replication in salivary gland cells (Fig. 1F and fig. S3, E and F).

We further investigated the role of USP8 in endoreplication progression in the *Bombyx* silk gland. Using the binary transgenic CRISPR-Cas9 system (*7*, *39*), we established *Bombyx* somatic mutants with heterozygous *USP8* mutations in the posterior silk gland (PSG) by crossing a line expressing Cas9 under the control of the PSG-specific *FibH* promoter with another line ubiquitously expressing a specific guide RNA (gRNA) targeting *USP8*. Subsequent sequencing analyses revealed that *USP8* mutations were caused by genomic deletions or insertions at the target site (fig. S4A), leading to reduced USP8 expression in the PSG at the transcriptional and translational levels, compared to the wild type (fig. S4, B and C). Notably, *USP8* mutation in the PSG decreased PSG size and the expression of three genes encoding PSG-specific silk proteins, namely, *FibH*, *FibL*, and *P25* (Fig. 1G and fig. S4D), resulting in thin cocoons with low silk production (Fig. 1G). However, *USP8* mutation in the PSG did not change body size, body weight, or developmental progression of *Bombyx* larvae (fig. S4, E to G). Moreover, like *USP8* knockdown in the *Drosophila* salivary gland, *USP8* mutation in the *Bombyx* PSG also reduced the *C* value and DNA content of PSG cells (Fig. 1, H and I) and abrogated DNA replication (Fig. 1J). Together, our data demonstrate that the deubiquitinase USP8 is required for endoreplication progression and growth of the *Drosophila* salivary gland and *Bombyx* silk gland.

USP8 deubiquitinates and stabilizes Fzr

Given that Fzr initiates the mitotic-to-endoreplication transition and cooperates with other cell cycle regulators to mediate the oscillation of DNA re-replication during endoreplication (*1*, *2*, *7*, *14*–*17*), we wondered whether the deubiquitinase USP8 could target Fzr and/or other cell cycle regulators to maintain their protein stability during endoreplication in *Bombyx* and *Drosophila*. To assess this possibility, we examined the effect of overexpressed USP8 on the protein levels of both Fzr and other cell cycle regulators, including CycE, Myc, and MCM6, three factors involved in endoreplication (*16*, *25*, *42*, *43*), in both *Bombyx* BmE cells and *Drosophila* S2 cells. Hemagglutinin (HA)–tagged USP8 was co-overexpressed with Flag-tagged Fzr or other regulators in these two cell lines. Subsequent Western blotting revealed that *USP8* overexpression increased the protein level of exogenously overexpressed Fzr in cultured cells (Fig. 2, A and B) but did not affect the protein levels of exogenously overexpressed CycE, Myc, or MCM6 (fig. S5, A to C), indicating that Fzr might be a specific target of USP8. Therefore, we further investigated the regulation of USP8 on Fzr protein levels in the *Bombyx* PSG and *Drosophila* salivary gland. First, reverse transcription quantitative polymerase chain reaction (RT-qPCR) and immunostaining analyses showed that *Fzr* expression had no obvious change at the mRNA level but accumulated at the protein level in the *Bombyx* PSG during the mitosis-to-endoreplication transition from stage 24 to stage 26 of embryonic development (fig. S5, D and E), suggesting that the Fzr protein may be regulated at the posttranslational level. USP8 was up-regulated in the *Bombyx* PSG during the mitosis-to-endoreplication transition at both mRNA and protein levels (fig. S5, F and G), showing a dynamic similar to Fzr protein levels. Second, we found that compared to the control, both *USP8* mutation in the *Bombyx* PSG and *USP8* knockdown in the *Drosophila* salivary gland substantially reduced the Fzr protein level (Fig. 2, C and D) but did not alter *Fzr* mRNA expression (fig. S5, H and I). Third, previous studies in *Drosophila* reported that APC/C^{Fzr} directly mediates the degradation of several cell cycle regulators such as CycA and CycB, two cyclins that their abnormal accumulation correlates with endoreplication arrest (*15*, *26*, *27*), and indirectly promotes the transcription of Myc, which thereby inhibits *CycB* transcription but positively regulates the transcription of MCM6 involved in DNA replication (*16*, *42*, *43*). Our investigation in the PSGs and salivary glands showed that USP8 depletion not only caused an accumulation of both CycA and CycB (fig. S5J) but also induced a decrease in

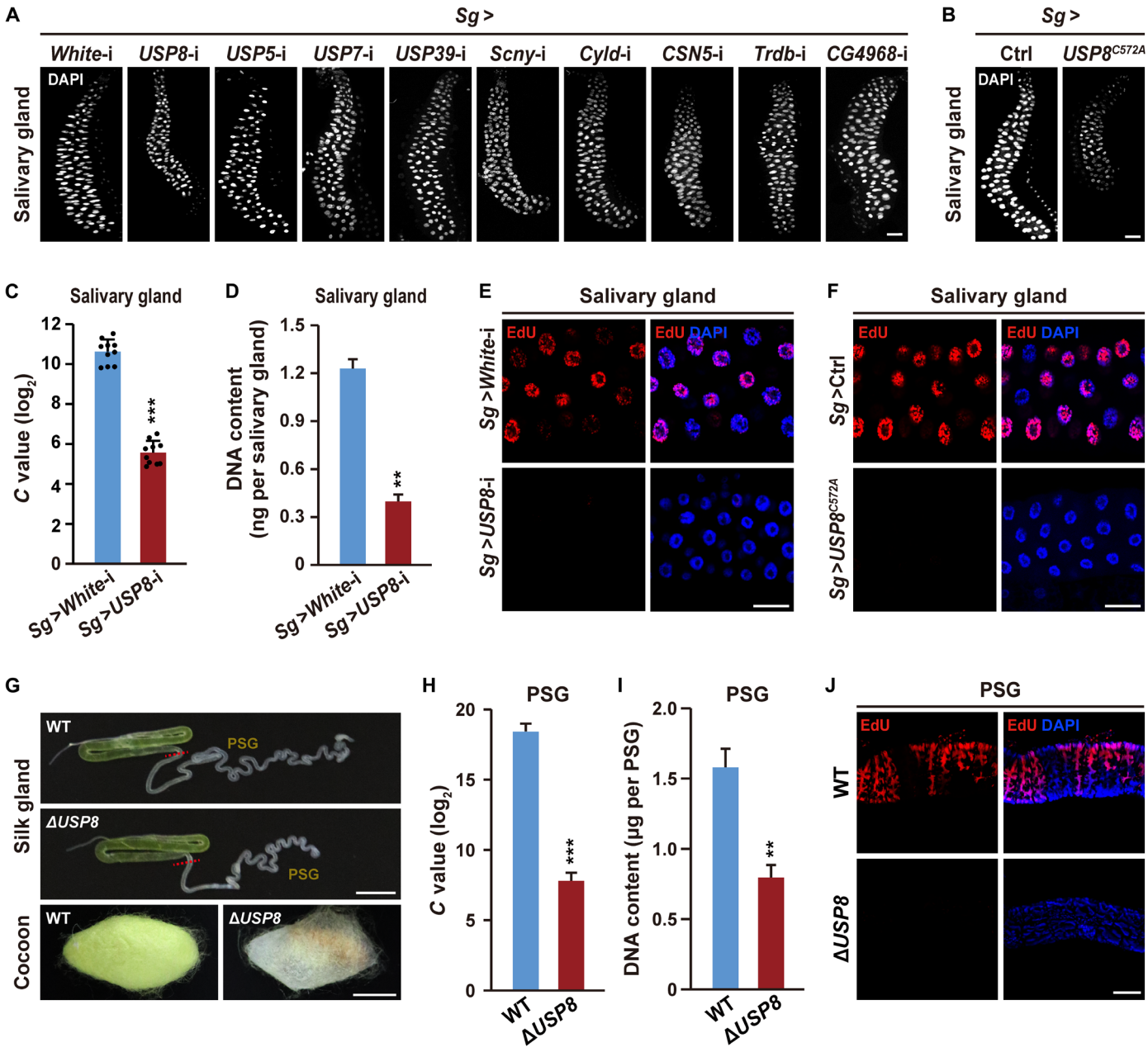

Fig. 1. Depletion of the deubiquitinase USP8 in the *Drosophila* salivary glands and *Bombyx* PSGs blocks endoreplication progression. (**A**) RNAi screening of deubiquitinases in the *Drosophila* salivary gland revealed that the knockdown of only *USP8* decreased gland size. Salivary glands were dissected at 120 hours AEL. Scale bar, 200 μm. (**B**) Overexpression of dominant-negative $USP8^{C572A}$ in the salivary gland decreased gland size at 120 hours AEL. Scale bar, 200 μm. (**C** and **D**) Salivary gland–specific *USP8* knockdown reduced the *C* value and DNA content in the salivary gland at 120 hours AEL. (**E** and **F**) EdU staining analyses of the effects of either *USP8* knockdown (E) or $USP8^{C572A}$ overexpression (F) on DNA replication in the salivary gland at 96 hours AEL. Scale bar, 50 μm. (**G**) CRISPR-Cas9–mediated *USP8* mutation in the *Bombyx* PSGs resulted in a decrease in PSG size at just wandering and thin cocoon with low silk production. Scale bars, 1 cm. (**H** and **I**) PSG-specific *USP8* mutation decreased the *C* value and DNA content in PSG cells at just wandering. (**J**) EdU staining revealed that PSG-specific *USP8* mutation blocked DNA replication in PSG cells at the second day of the fourth larval instar. Scale bar, 50 μm. i, RNAi; AEL, after egg laying; WT, wild type. The data are presented as the mean ± SE (error bars) of three independent biological replicates. For the significance test: $^{**}P < 0.01$ and $^{***}P < 0.001$ versus the control.

the transcription of *Myc* and *MCM6* but an increase in *CycB* transcription (fig. S5, K and L). Collectively, these results suggest that USP8 positively regulates Fzr protein levels.

We then investigated whether USP8 regulates the Fzr protein level by modulating Fzr protein stability through deubiquitination. First, we measured the changes in Fzr protein levels following treatment with cycloheximide (CHX), an inhibitor of protein synthesis. Pulse-chase experiments revealed that CHX treatment decreased the protein levels of endogenous Fzr in ex vivo–cultured PSGs and salivary glands and exogenously overexpressed Fzr in BmE cells and S2 cells in a time-dependent manner (Fig. 2E and fig. S6A), indicating a degradation of the Fzr protein in the presence of

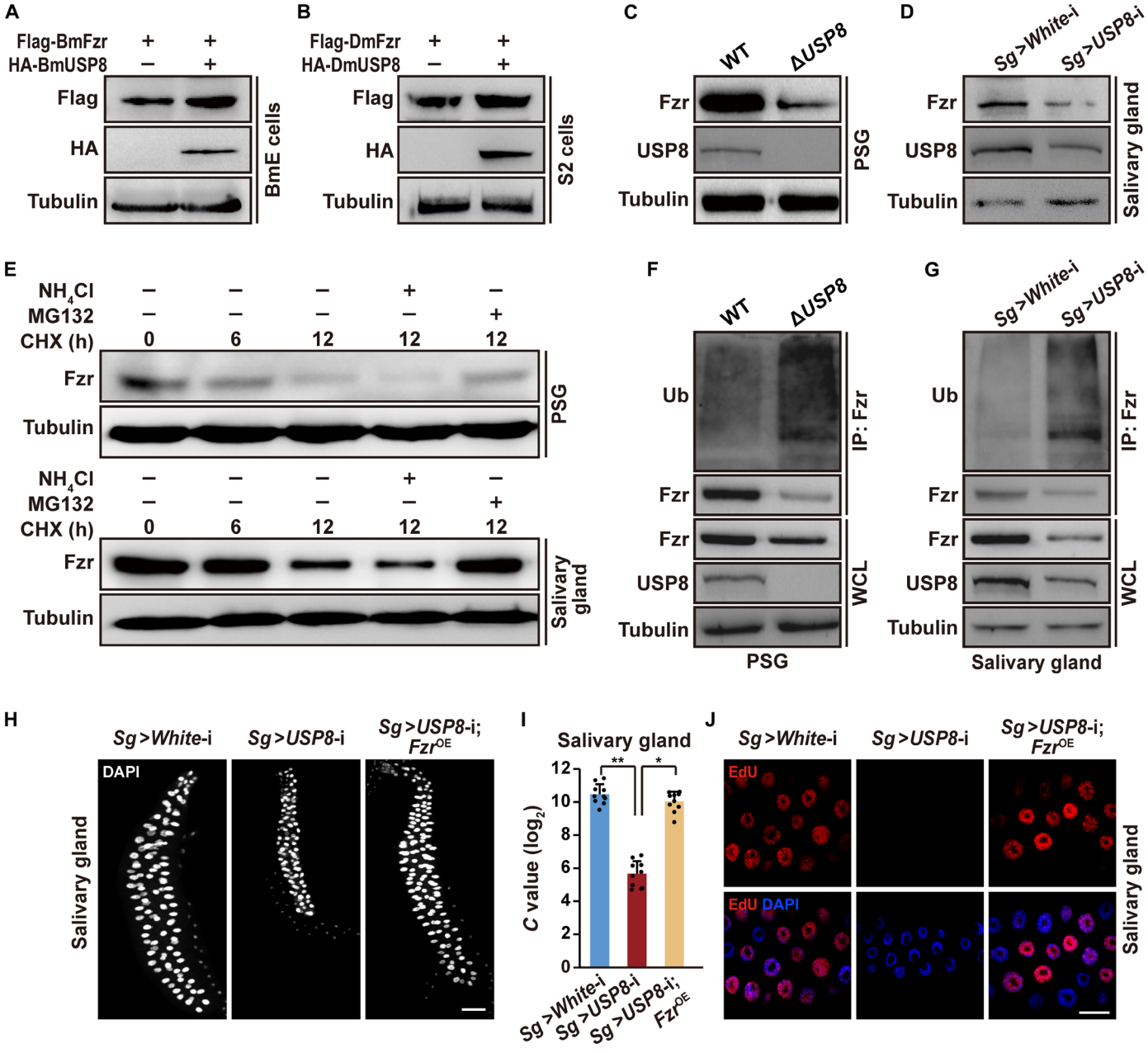

Fig. 2. USP8 stabilizes Fzr through deubiquitination. (**A** and **B**) *USP8* overexpression in *Bombyx* BmE cells and *Drosophila* S2 cells increased Fzr protein levels. (**C** and **D**) USP8 depletion in the *Bombyx* PSGs and *Drosophila* salivary glands decreased Fzr protein levels. (**E**) Fzr protein levels in the PSGs and salivary glands were reduced by CHX treatment, and this reduction was reversed by simultaneous MG132 treatment. (**F** and **G**) USP8 depletion in the PSGs and salivary glands increased Fzr ubiquitination. (**H** to **J**) *Fzr* overexpression in the salivary gland reversed the effects of *USP8* knockdown on the gland size, the *C* value, and DNA replication during endoreplication. Salivary glands were dissected at 120 hours AEL for size and *C* value measurement and were dissected at 96 hours AEL for EdU staining and RT-qPCR. Scale bars, 200 μm (H) and 50 μm (J). OE, overexpression; Bm, *Bombyx*; Dm, *Drosophila*; WCL, whole cell lysate; h, hours. The data are presented as the mean ± SE (error bars) of three independent biological replicates. For the significance test: $*P < 0.05$ and $**P < 0.01$ versus the control.

CHX. In general, protein degradation is mediated by the ubiquitin-proteasome pathway and the autophagy-lysosome pathway (*44*, *45*). We found that the degradation of the Fzr protein was suppressed by the proteasome inhibitor MG132 but not by the lysosome inhibitor NH_4Cl (Fig. 2E and fig. S6A), indicating that Fzr protein instability is driven by the ubiquitin-proteasome pathway. Moreover, we observed that in BmE cells and S2 cells, *USP8* overexpression inhibited the degradation of exogenously overexpressed Fzr protein in the presence of CHX (fig. S6B). Notably, in vivo ubiquitination assays showed that USP8 depletion in the *Bombyx* PSGs and *Drosophila* salivary glands increased Fzr ubiquitination levels (Fig. 2, F and G, and fig. S6, C and D); *USP8* overexpression in BmE cells or S2 cells reduced the ubiquitination of exogenously overexpressed Fzr (fig. S6E); and the treatment with the USP8-specific inhibitor IN-2

increased the ubiquitination of overexpressed Fzr protein (fig. S6F). These results suggest that USP8 maintains Fzr stability by inhibiting Fzr ubiquitination and degradation, which is mediated by the ubiquitin-proteasome pathway.

Epistatic analysis in *Drosophila* revealed that compared to the effects of salivary gland–specific *USP8* knockdown, *Fzr* overexpression in the salivary gland with *USP8* knockdown not only reversed the decrease in gland size and DNA content caused by *USP8* knockdown (Fig. 2, H and I) but also reinitiated DNA replication (Fig. 2J) and reversed the abnormality in the expression of three genes downstream of Fzr during endoreplication, including *Myc*, *MCM6*, and *CycB* (fig. S7A). In addition, we observed that salivary gland–specific *Fzr* overexpression had no effect on the gland size and the *C* value of gland cells compared to the control, and *USP8* knockdown in the salivary gland with *Fzr* overexpression also did not change the gland size and the *C* value (fig. S7, B and C). These findings further indicate that USP8 maintains Fzr stability during endoreplication. Together, our data reveal that USP8 regulates endoreplication by functioning as a Fzr deubiquitinase to stabilize Fzr through deubiquitination.

USP8 physically interacts with Fzr

Deubiquitinases generally interact with substrate proteins and subsequently mediate their deubiquitination (*29*, *30*, *33*). Given that Fzr proteins from *Bombyx* and *Drosophila* contain different numbers of WD40 domains that mediate protein-protein interaction, we thus investigated whether USP8 interacts with Fzr. First, on the basis of in silico predication using the AlphaFold 3 program (*46*), we observed that some amino acid residues within several WD40 domains of *Bombyx* and *Drosophila* Fzr proteins exhibited potential binding with specific amino acid residues of USP8 proteins via hydrogen bonds (fig. S8), indicating a potential interaction between USP8 and Fzr. Second, to determine whether USP8 interacts with Fzr in vivo, we co-overexpressed HA-tagged USP8 and Flag-tagged Fzr in *Bombyx* BmE cells and *Drosophila* S2 cells and then conducted coimmunoprecipitation (co-IP) experiments with specific antibodies. The results showed that exogenously overexpressed USP8 and Fzr reciprocally coimmunoprecipitated (Fig. 3, A and B, and fig. S9, A and B). Similarly, further co-IP experiments confirmed the interaction between endogenous USP8 and Fzr in cultured BmE cells and S2 cells (Fig. 3C and fig. S9C) as well as in the *Bombyx* PSGs and *Drosophila* salivary glands (Fig. 3D and fig. S9D). Third, glutathione *S*-transferase (GST) pull-down assays revealed that bacterially purified recombinant Trx-His–tagged USP8 interacted with recombinant GST-tagged Fzr in vitro (fig. S9, E and F). Collectively, these data demonstrate that USP8 physically interacts with Fzr.

Given that USP8 contains a ubiquitin C-terminal hydrolase (UCH) domain at the C terminus and a dimerization domain at the N terminus (*47*), we investigated which of these domains might be involved in the USP8-Fzr interaction. We generated two constructs for overexpressing two USP8 truncation mutants, one containing the UCH domain but lacking the dimerization domain (USP8-C) and the other containing the dimerization domain but lacking the UCH domain (USP8-N), in both BmE cells and S2 cells. Subsequent reciprocal co-IP assays showed that unlike USP8-N, USP8-C could not coimmunoprecipitate with Fzr (Fig. 3, E and F, and fig. S9, G and H), suggesting that the dimerization domain of USP8 is necessary for its interaction with Fzr. Furthermore, to determine which of WD40 domains in Fzr proteins might be involved in the USP8-Fzr interaction, we generated a series of constructs for overexpressing truncated Fzr with the deletion of single WD40 domain and then performed co-IP assays in cultured cells. The results revealed that the second and third WD40 domains of *Bombyx* Fzr were required for its interaction with USP8 (Fig. 3G), while the second and fifth WD40 domains of *Drosophila* Fzr were required for its interaction with USP8 (Fig. 3H). These results were consistent with the AlphaFold 3–based prediction, further confirming that different WD40 domains of Fzr proteins mediate the interaction of Fzr with USP8 in *Bombyx* and *Drosophila*.

Hsp70 promotes the interaction between USP8 and Fzr

Since the interaction between USP8 and Fzr indicated by in vitro GST pull-down assays (fig. S9, E and F) was relatively slight compared to that shown by in vivo co-IP assays (Fig. 3), we speculated that other cofactors may modulate the USP8-Fzr interaction. To this end, we reanalyzed the Fzr interactome characterized by mass spectrometry analysis in our previous study (*16*) and selected the molecular chaperone Hsp70 among potential Fzr-interacting partners as a candidate of interest, because the Hsp70 chaperone network plays indispensable roles in the folding, assembly, stabilization, or degradation of cellular proteins (*48*–*51*). First, AlphaFold 3–based analysis predicted that some amino acid residues within several WD40 domains of Fzr proteins from *Bombyx* and *Drosophila* had potential binding with specific amino acid residues of Hsp70 proteins via hydrogen bonds (fig. S10, A and B), indicating a potential interaction between Hsp70 and Fzr. Second, we validated the interaction between Hsp70 and Fzr in vivo and in vitro in detail. Reciprocal co-IP experiments revealed that exogenously overexpressed V5-tagged Hsp70 could interact with Flag-tagged Fzr in *Bombyx* BmE cells and *Drosophila* S2 cells (Fig. 4, A and B, and fig. S11, A and B). Similarly, we observed an interaction between endogenous Hsp70 and Fzr in BmE cells, S2 cells, the *Bombyx* PSGs, and the *Drosophila* salivary glands (Fig. 4, C and D, and fig. S11, C and D). In addition, GST pull-down assays also confirmed a direct interaction between Hsp70 and Fzr in vitro (fig. S11, E and F). Third, we assessed the effect of treatment with 2-phenylethynesulfonamide (PES), an inhibitor that hinders the interactions between Hsp70 and its partners (*52*), on the Hsp70-Fzr interaction. As expected, co-IP experiments revealed that PES treatment for 2 hours not only impaired the interaction between exogenously overexpressed V5-tagged Hsp70 and Flag-tagged Fzr in BmE cells and S2 cells (fig. S11G) but also inhibited the interaction between endogenous Hsp70 and Fzr in BmE cells, S2 cells, PSGs, and salivary glands (Fig. 4E and fig. S11H). Collectively, these data clearly confirmed a physical interaction between Hsp70 and Fzr.

Given that the Hsp70 protein contains two conserved domains, a nucleotide-binding domain (NBD) for binding and hydrolyzing adenosine triphosphate and a substrate-binding domain (SBD) for interacting with target proteins (*48*, *53*), we investigated which of these two domains might be involved in the Hsp70-Fzr interaction. Several plasmids for overexpressing Hsp70 truncations with the deletion of the SBD ($Hsp70^{\Delta SBD}$) or the NBD ($Hsp70^{\Delta NBD}$) were constructed and then separately cotransfected with the *Fzr* overexpression construct into BmE cells and S2 cells. Subsequent reciprocal co-IP experiments showed that, unlike NBD deletion, SBD deletion blocked the interaction of Hsp70 with Fzr (Fig. 4F and fig. S11I), indicating that Hsp70 interacts with Fzr through its SBD. In addition, we accessed which WD40 domain of Fzr protein will be essential for the interaction of Fzr with Hsp70. Combining truncation approach and co-IP assays in cultured cells, we found that the second and third WD40 domains of *Bombyx* Fzr while the fourth, sixth, and seventh

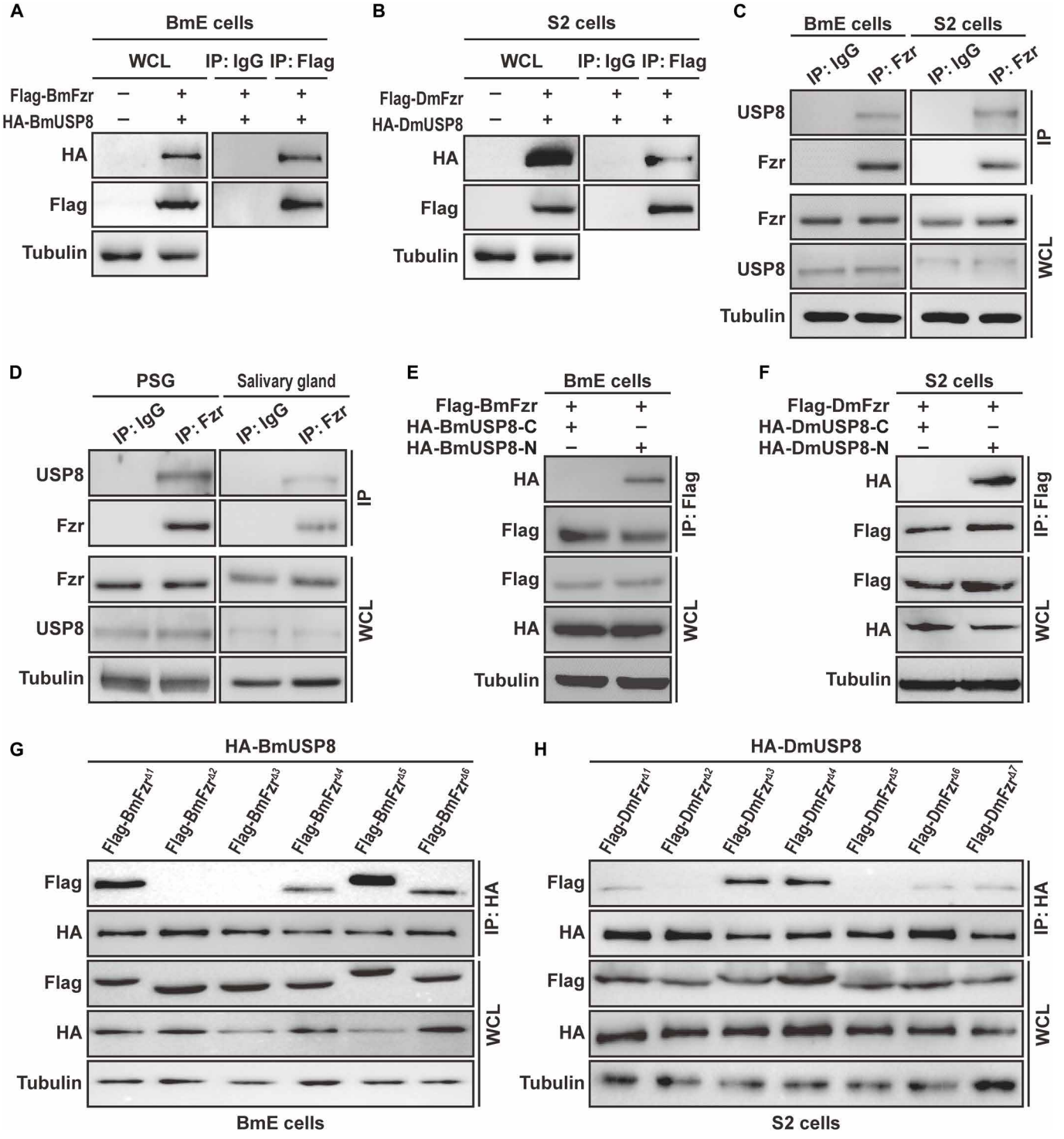

Fig. 3. USP8 interacts with Fzr. (**A** and **B**) Co-IP assays with an anti-Flag antibody revealed that exogenously overexpressed HA-tagged USP8 interacted with Flag-tagged Fzr in both *Bombyx* BmE cells and *Drosophila* S2 cells. (**C** and **D**) Co-IP assays with an anti-Fzr antibody revealed that endogenous USP8 in cultured cells and glands interacted with endogenous Fzr. (**E** and **F**) Co-IP assays with an anti-Flag antibody confirmed that the deletion of the dimerization domain of USP8 (USP8-C), not the UCH domain (USP8-N), blocked the interaction of USP8 with Fzr in cultured cells. (**G** and **H**) Truncation experiment followed by co-IP assay with an anti-HA antibody revealed that several WD40 domains of Fzr were essential for the interaction of Fzr with USP8. The number indicated the deletion of corresponding WD40 domain of Fzr. IgG, immunoglobulin G.

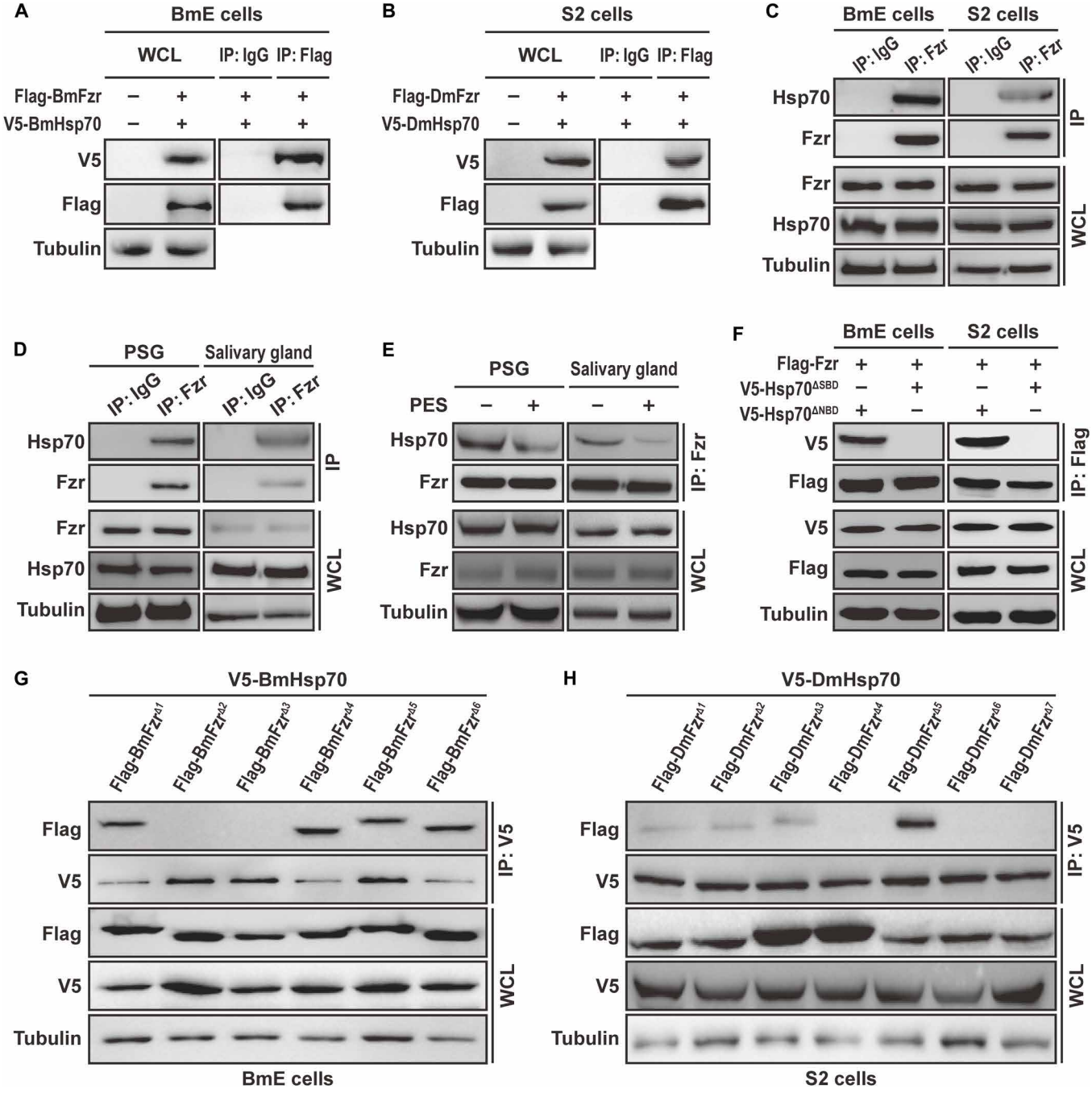

Fig. 4. Hsp70 interacts with Fzr. (**A** and **B**) Co-IP assays with an anti-Flag antibody revealed that exogenously overexpressed V5-tagged Hsp70 interacted with Flag-tagged Fzr in both *Bombyx* BmE cells and *Drosophila* S2 cells. (**C** and **D**) Co-IP assays with an anti-Fzr antibody revealed that endogenous Hsp70 interacted with endogenous Fzr in cultured cells, the *Bombyx* PSGs, and *Drosophila* salivary glands. (**E**) Co-IP assays with an anti-Fzr antibody confirmed that the treatment with the Hsp70 inhibitor PES attenuated endogenous Hsp70-Fzr interaction in the PSGs and salivary glands. (**F**) Co-IP assays with an anti-Flag antibody confirmed the deletion of the SBD domain of Hsp70, not NBD domain, blocked the interaction of Hsp70 with Fzr in cultured cells. Hsp70 and Fzr from both *Bombyx* and *Drosophila* were separately analyzed in corresponding cells. SBD, substrate-binding domain. NBD, nucleotide-binding domain. (**G** and **H**) Truncation experiment followed by co-IP assay with an anti-V5 antibody revealed that several WD40 domains of Fzr were essential for the interaction of Fzr with Hsp70. The number indicated the deletion of corresponding WD40 domain of Fzr.

WD40 domains of *Drosophila* Fzr were essential for the interaction of Fzr with Hsp70 (Fig. 4, G and H). This is consistent with the observation from AlphaFold 3–based prediction of the interaction between Hsp70 and Fzr.

We next investigated whether Hsp70 is associated with the USP8-Fzr interaction. Co-IP experiments showed that *Hsp70* overexpression promoted the interaction between exogenously overexpressed USP8 and Fzr in BmE cells and S2 cells (Fig. 5, A and B). Similarly, GST pull-down assays confirmed that Hsp70 supplementation enhanced the USP8-Fzr interaction (Fig. 5, C and D). Furthermore, we examined the change of the USP8-Fzr interaction following treatment for 2 hours with PES as a Hsp70 activity inhibitor. The results showed that PES treatment attenuated the interaction between endogenous USP8 and Fzr in ex vivo–cultured PSGs and salivary glands (Fig. 5, E and F) as well as in BmE cells and S2 cells (Fig. 5, G and H). Moreover, we investigate possible mechanism by which Hsp70 facilitates the USP8-Fzr interaction. Hsp70 mainly plays chaperone activity to promote proper folding of its substrate proteins (*48*–*51*), and properly folded proteins are capable of interacting selectively with their partners (*54*, *55*). Given that the luciferase enzyme activity of a protein fused with luciferase has been widely used to define the status of proper folding of this protein in vivo (*56*–*58*), we therefore analyzed Hsp70 regulation of Fzr folding by assessing the effect of impairing the Hsp70 chaperone activity or overexpressing *Hsp70* on the luciferase enzyme activity of recombinant Fzr-Luc protein in BmE and S2 cells. The results showed that compared to the control, the treatments with PES or VER155008, two specific inhibitors that target the Hsp70 chaperone activity by separately inhibiting the interacting activity or enzymatic activity of Hsp70 (*52*, *59*), decreased the Fzr-Luc luciferase activity (Fig. 5, I and J, and fig. S12, A and B). In addition, we observed that overexpression of intact *Hsp70* increased the Fzr-Luc luciferase activity compared to the control (Fig. 5, K and L, and fig. S12, C and D), but truncated Hsp70 with the deletion of either SBD domain or NBD domain lost this promotion (Fig. 5, K and L, and fig. S12, C and D). Together, our data suggest that Hsp70 mediates proper folding of Fzr, thereby promoting the interaction of Fzr with USP8.

Hsp70 regulates endoreplication by promoting Fzr deubiquitination and stabilization

To explore the physiological functions of Hsp70 during endoreplication, we conducted tissue-specific depletion of Hsp70 in the *Bombyx* PSG and *Drosophila* salivary gland. First, we used the CRISPR-Cas9 system to mutate the *Hsp70* gene in the *Bombyx* PSG (fig. S13, A to C). The results revealed that *Hsp70* mutation decreased the size of silk gland and disrupted the formation of cocoons as well as the expression of silk protein genes (Fig. 6A and fig. S13D) but did not affect body size, body weight, or developmental progression of *Bombyx* larvae (fig. S13, E to G). Similarly, we observed that RNAi-mediated *Hsp70* knockdown in the *Drosophila* salivary gland substantially reduced gland size (Fig. 6B and fig. S13H) but had no effect on body size and developmental progression (fig. S13, I to K). We noted that Hsp70 depletion in both the PSGs and salivary glands reduced the *C* value in gland cells (fig. S14, A and B) and abrogated DNA replication (Fig. 6, C and D). These data demonstrate that Hsp70 is functionally required for endoreplication progression in the PSG and salivary gland.

We next investigated the regulation of Hsp70 on Fzr stability during endoreplication. First, RT-qPCR and immunostaining analyses revealed that the mRNA and protein expressions of Hsp70 were upregulated in the *Bombyx* PSGs during the mitotic-to-endoreplication transition from stage 24 to stage 26 of embryonic development (fig. S15, A and B), being consistent with the dynamics of Fzr protein levels (fig. S5E). Second, we found that similar to the effects of USP8 depletion, Hsp70 depletion in both the PSGs and salivary glands decreased Fzr protein levels but did not change the *Fzr* mRNA levels in these two types of glands (Fig. 6E and fig. S16, A and B). In addition, Hsp70 depletion also disturbed Fzr downstream signaling by leading to an accumulation of two Fzr substrate proteins CycA and CycB (fig. S16C) and a dysregulation of mRNA expressions for three genes that are transcriptionally modulated by Fzr, including *Myc*, *MCM6*, and *CycB* in the glands (fig. S16, D and E). Notably, our analyses in both BmE cells and S2 cells showed that *Hsp70* overexpression elevated the protein levels of exogenously overexpressed Fzr but not other endoreplication-related factors, including CycE, Myc, and MCM6 (Fig. 6F and fig. S16, F to H); in the presence of the protein synthesis inhibitor CHX, *Hsp70* overexpression inhibited the CHX-induced decrease in Fzr protein levels (fig. S16I). These results indicate that Hsp70 is required for the stabilization of Fzr. Third, we examined whether Hsp70 maintains Fzr stability by decreasing ubiquitination levels of Fzr. To this end, we performed ubiquitination assays and observed that Hsp70 depletion elevated ubiquitination levels in the PSGs and salivary glands (Fig. 6G and fig. S16J). In contrast, *Hsp70* overexpression in cultured cells decreased ubiquitination levels of the exogenously overexpressed Flag-Fzr protein (fig. S16K); in cultured cells and ex vivo cultured glands, treatment with the Hsp70 activity inhibitor PES for 6 hours led to a decrease in Fzr protein levels and an increase in Fzr ubiquitination levels (fig. S17, A and B) but did not change *Fzr* mRNA expression (fig. S17, C to F). These results suggest that Hsp70 stabilizes Fzr through deubiquitination.

We then conducted epistatic analysis in *Drosophila* and observed that, compared to salivary gland–specific *Hsp70* knockdown, *Fzr* overexpression in the salivary gland with *Hsp70* knockdown reversed the defects caused by *Hsp70* knockdown, including a decrease in gland size (Fig. 6H), abrogation of DNA replication (Fig. 6I), reduction in DNA content (fig. S18A), and dysregulation of the expression for three genes downstream of Fzr during endoreplication, including *Myc*, *MCM6*, and *CycB* (fig. S18B). Furthermore, we noted that salivary gland–specific *Fzr* overexpression had no effect on the gland size and the *C* value of gland cells compared to the control, and *Hsp70* knockdown in the salivary gland with *Fzr* overexpression also did not change the gland size and the *C* value (fig. S18, C and D). These data further indicate that Hsp70 is involved in the maintenance of Fzr stability during endoreplication. Collectively, our findings reveal that Hsp70 regulates endoreplication by promoting the USP8-Fzr interaction and subsequently modulating Fzr deubiquitination and stabilization.

The USP8-Hsp70-Fzr axis is not essential for mitotic progression

Previous studies have demonstrated that Fzr is concentrated at centrosomes throughout the cell cycle and mediates cyclin removal during G_1 phase in mitotic cells in *Drosophila* (*15*, *16*, *26*, *60*–*62*). However, in *Drosophila* prothoracic gland cells and ovarian follicle cells that also occur the mitosis-to-endoreplication transition, Fzr was shown to be unnecessary for mitotic cell cycle progression and cell proliferation before endoreplication entry (*10*, *14*, *63*). Thus, we further selected the *Drosophila* wing disc, a tissue that only undergoes mitotic cycle and has no endoreplication cycle, to test

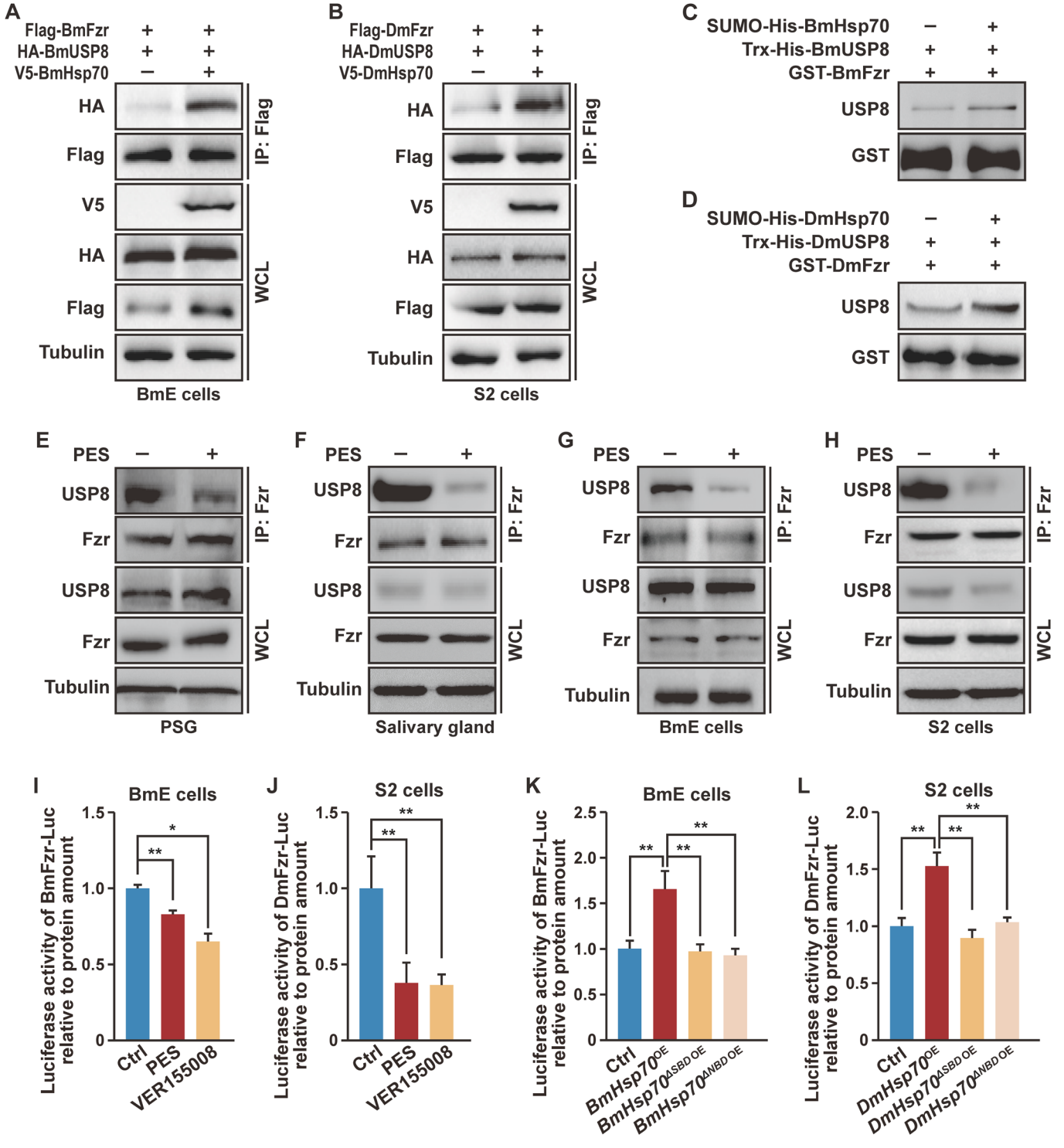

Fig. 5. Hsp70 promotes the interaction between Fzr and USP8 by mediating Fzr folding. (**A** and **B**) Exogenously overexpressed Hsp70 promoted the interaction between exogenously overexpressed USP8 and Fzr in BmE cells and S2 cells. (**C** and **D**) GST pull-down assay showed that supplementation with recombinant Hsp70 increased the USP8-Fzr interaction in vitro. (**E** to **H**) The interaction between endogenous USP8 and Fzr in the cultured glands and cells was attenuated following a treatment with the Hsp70 interacting activity inhibitor PES for 2 hours. (**I** and **J**) The treatment with the Hsp70 inhibitors PES or VER155008 decreased the luciferase enzyme activity of luciferase-fused Fzr (Fzr-Luc) in cultured cells, suggesting that Hsp70 promoted proper folding of Fzr. (**K** and **L**) Overexpression of intact *Hsp70* increased the luciferase enzyme activity of Fzr-Luc in cultured cells, but truncated Hsp70 with the deletion of SBD domain or NBD domain lost this promotion. The data are presented as the mean ± SE (error bars) of three independent biological replicates. For the significance test: $*P < 0.05$ and $**P < 0.01$ versus the control.

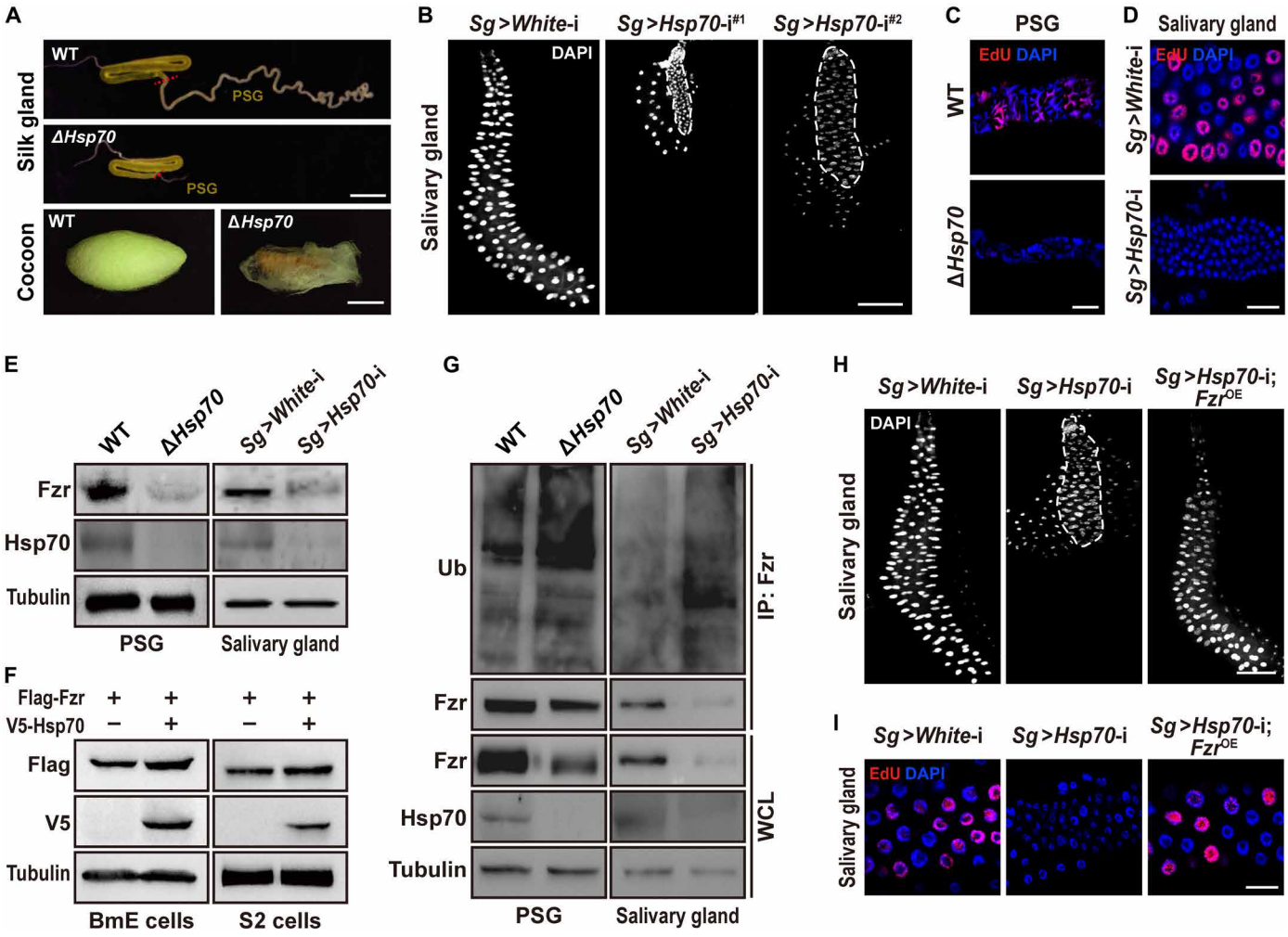

Fig. 6. Hsp70 regulates endoreplication by maintaining Fzr stability. (**A**) CRISPR-Cas9–mediated *Hsp70* mutation in the *Bombyx* PSG decreased PSG size at just wandering and affected cocoon formation. Scale bar, 1 cm. (**B**) *Hsp70* knockdown in the *Drosophila* salivary gland reduced gland size at 120 hours AEL. Scale bar, 200 μm. (**C** and **D**) Hsp70 depletion blocked DNA replication in the PSGs at the second day of the fourth larval instar and salivary glands at 96 hours AEL. Scale bars, 50 μm. (**E**) Hsp70 depletion in the PSGs and salivary glands decreased the Fzr protein level in two glands. (**F**) Exogenously overexpressed Hsp70 in cultured cells increased the protein level of exogenously overexpressed Fzr. Hsp70 and Fzr from both *Bombyx* and *Drosophila* were separately analyzed in corresponding cells. (**G**) Hsp70 depletion elevated Fzr ubiquitination in the PSGs and salivary glands. (**H** and **I**) *Fzr* overexpression in the salivary gland reversed the effects of *Hsp70* knockdown on gland size at 120 hours AEL and DNA replication at 96 hours AEL. Scale bars, 200 μm (H) and 50 μm (I).

whether the USP8-Hsp70-Fzr axis is involved in the control of mitotic progression. We carried out RNAi-mediated knockdown of genes from the USP8-Hsp70-Fzr axis in the *Drosophila* wing disc using the *Nubbin*-Gal4 driver. The results showed that compared to the control, wing disc–specific *Fzr* knockdown had no obvious effect on the size of the wing disc (fig. S19A). In addition, EdU incorporation assay and phospho-histone 3 (pH3) staining revealed no change in DNA replication and cell proliferation in wing disc cells followed by *Fzr* knockdown, respectively (fig. S19, B and C), indicating that Fzr is also not involved in mitotic progression in the wing disc. Similarly, we found that the knockdown of either *USP8* or *Hsp70* did not alter wing disc size as well as DNA replication and cell proliferation in wing disc cells (fig. S19, A to C). Collectively, our data, together with previous findings regarding of Fzr roles in *Drosophila*, suggest that the USP8-Hsp70-Fzr axis is essential for endoreplication cycle but not for mitotic progression.

DISCUSSION

Endoreplication is a cell cycle variant that arises from mitotic exit and involves multiple rounds of DNA replication without mitosis, thereby contributing to the growth and final size of cells and tissues in animals and plants (*1*, *2*). Fzr in insects and its homologs in mammals and plants have been shown to function as a master regulator in the control of the mitosis-to-endoreplication transition and endoreplication maintenance (*1*, *2*, *4*, *18*, *21*). However, how Fzr protein stability is regulated remains unclear. Here, through genetic screening, we found in the *Drosophila* salivary gland and *Bombyx* silk gland, two well-understood endoreplicating tissues in insects, that the deubiquitinase USP8 and the molecular chaperone Hsp70 regulate the endoreplication cycle by synergistically promoting the deubiquitination and stabilization of Fzr; disrupting this signaling cascade reduces the growth and the final size of endoreplicating glands (fig. S20), thereby affecting physiological functions of glands,

such as silk production in the silk gland. Our data uncover a previously unanticipated role for USP8 and Hsp70 in maintaining Fzr protein stability and establish deubiquitination-dependent regulation of the endoreplication cycle.

Ubiquitination and deubiquitination, two reversible posttranslational modifications that are separately governed by ubiquitin E3 ligases and deubiquitinases, have opposite effects on the stability of substrate proteins (*29*–*33*). Previous reports in the *Drosophila* salivary gland have focused on the role of the ubiquitination cascade in sustaining the endoreplication cycle. Fzr activates the E3 ubiquitin ligase APC/C to mediate ubiquitination and subsequent degradation of cyclins and other cell cycle factors during endoreplication (*1*, *2*), and APC/C^{Fzr}-mediated endoreplication progression depends on a molecular oscillator composing of transcription factor E2F1, CycE-Cdk2, APC/C^{Fzr}, and E3 ubiquitin ligases $CRL4^{Cdt2}$ (*1*, *2*, *25*). In this oscillator, elevated CycE-Cdk2 activity by accumulated E2F1 in late G phase suppresses APC/C^{Fzr} activity and drives S phase entry; during S phase, activated $CRL4^{Cdt2}$ degrades E2F1 to induce a drop in the CycE-Cdk2 activity, thereby reestablishing a G phase and allows high APC/C^{Fzr} activity; APC/C^{Fzr} degrades geminin to facilitate PreRC assembly for the next cycle. The present study identified USP8 as a bona fide deubiquitinase that directly deubiquitinates and stabilizes Fzr through a physical interaction in the *Drosophila* salivary gland and *Bombyx* silk gland, which delineates essential role for the deubiquitination cascade in the maintenance of endoreplication progression and unravels another regulatory layer of protein homeostasis during endoreplication. In addition, USP8 regulation of endoreplication progression at the posttranslational level also differs with the roles of several unknown regulators or signaling pathways, such as E2F1 (*25*, *64*), Myc (*16*, *42*, *43*), Cut (*65*), the Notch pathway (*14*, *17*, *65*, *66*), the mechanistic target of rapamycin (mTOR) pathway (*9*, *67*), and the hormone pathway (*11*, *68*), which mainly function at the transcriptional level. Given that the APC/C^{Fzr} activity must oscillate and need a drop in late G phase to sustain endoreplication cycles (*1*, *2*), hence it will be intriguing to explore whether Fzr can be targeted and degraded by a specific ubiquitin ligase during endoreplication.

The Hsp70 chaperone network generally acts to maintain protein homeostasis by mediating proper folding of nascent proteins, protein translocation, the assembly and disassembly of protein complexes, the prevention of protein aggregation, and the degradation of aberrant proteins and protein aggregates, through protein-protein interactions (*48*–*51*). In our previous study, Hsp70 was shown to be a potential Fzr interacting partner (*16*). Here, we demonstrated that Hsp70 regulates endoreplication progression in the salivary gland and silk gland by interacting with Fzr to modulate its deubiquitination and stabilization. Mechanistically, Hsp70 appears to monitor proper folding of Fzr protein and promote its interaction with USP8. Since proper folding of proteins generally devotes to their interactions with other partners (*54*), like the WD40 protein Bub3 (*55*), we thus suggest that the interaction of Hsp70 with Fzr facilitates proper folding of Fzr, thereby enhancing the interaction of Fzr with USP8 to promote Fzr deubiquitination and stabilization during endoreplication. In addition, because Hsp70 belongs to the heat shock protein family that generally responds to heat stress (*69*), it also raised another question about a potential impact of heat stress on the regulation of Fzr by Hsp70. Our preliminary analyses showed that compared to normal growth temperature of 27°C for cultured cells or 25°C for insect individuals, intermittent higher temperature treatment under 37°C obviously elevated protein levels of both Fzr and Hsp70 in cultured cells as well as in both the *Bombyx* PSGs and *Drosophila* salivary glands (fig. S21, A to D), lastly leading to a death of *Bombyx* and *Drosophila* larvae (fig. S21E). However, higher temperature did not change gland size and DNA replication in gland cells (fig. S21, F to I). This observation is similar to the fact that *Fzr* overexpression does not promote endoreplication in the *Drosophila* salivary gland (figs. S7 and S18), speculating that heat stress has no effect on endoreplication progression. Together, our data conclude that Hsp70 plays its chaperone function, not heat response, in the regulation of endoreplication progression.

Endoreplication is an evolutionarily conserved mechanism for polyploidy formation as well as the growth of cell and tissue in animals and plants. Numerous studies have also shown that Fzr and its homologs play a conserved and indispensable role in the mitosis-to-endoreplication transition and endoreplication maintenance in multiple species, including *Drosophila* (*16*, *23*, *24*), *Bombyx* (*7*), *Nilaparvata* (*70*), *Mus* (*71*), and *Arabidopsis* (*20*). This study used the *Drosophila* salivary gland and *Bombyx* silk gland to unveil the regulation of USP8 and Hsp70 on Fzr protein stability and endoreplication progression, revealing that endoreplication control by the USP8-Hsp70-Fzr axis is evolutionarily conserved in insects to a certain extent. Whether this regulatory axis is also involved in endoreplication in other insects and vertebrates needs to be further explored.

MATERIALS AND METHODS

Drosophila stocks, *Bombyx* strain, and developmental timing

All *Drosophila* stocks were reared at 25°C on standard cornmeal medium under a 12-hour:12-hour light:dark cycle. The *UAS-White* RNAi (THU0558), *UAS-USP8* RNAi (THU3923), *UAS-Hsp70* RNAi (THU1250), *UAS-Fzr* RNAi (TH201500745.S), *UAS-USP5* RNAi (THU2262), *UAS-USP7* RNAi (THU3682), *UAS-Cyld* RNAi (THU5236), and *UAS-Scny* RNAi (THU5262) lines were obtained from the Tsinghua University Fly Center; the *UAS-USP39* RNAi (#7288R-1) and *UAS-CSN5* RNAi (#14884R-1) lines were obtain from National Institute of Genetics at Japan; the *UAS-White* RNAi line was used as the control. The *UAS-USP12* RNAi (V27799), *UAS-USP14* RNAi (V27405), *UAS-USP15* RNAi (V33726), *UAS-USP16* RNAi (V110286), *UAS-USP20* RNAi (V42609), *UAS-DUBAI* RNAi (V28960), *UAS-Josd* RNAi (V7113), *UAS-Trbd* RNAi (V330368), *UAS-CG4968* RNAi (V330332), V60000, and V60100 lines were obtained from the Vienna *Drosophila* Resource Center; because of the difference of the plasmids for line construction, V60000 or V60100 was used as the control for the former seven lines, and the *UAS-White* RNAi line was used as the control for the last two lines. The *UAS-Fzr* (F000893) line was obtained from FlyORF. The line carrying a dominant-negative form of *USP8* (*UAS-*$USP8^{C572A}$) was used to impair USP8 activity (*36*, *37*). The *UAS-GFP* (THJ0179) and the wild-type yw lines were obtained from the Tsinghua University Fly Center and Bloomington *Drosophila* Stock Center, respectively. The *UAS-GFP* and yw were used as the controls for the overexpression of *UAS-Fzr* and *UAS-*$USP8^{C572A}$, respectively. *Sg*-Gal4 was used to specifically drive gene expression in the *Drosophila* salivary gland (*40*). *Nubbin*-Gal4 was used to drive gene expression specifically in the *Drosophila* wing discs (*72*). The nondiapaused *Bombyx* strain D9L was used in the present study. Both the wild-type and transgenic *Bombyx* strains were fed with fresh mulberry leaves at 25°C with a 12-hour light:12-hour dark cycle.

Developmental timing was conducted as described previously (*73*). For *Drosophila*, the crossed flies laid eggs on standard diet for 4 hours at 25°C, and approximately 30 larvae were collected at 36 hours after egg laying (AEL) and were reared in a vial with standard diet at 25°C for developmental timing. For *Bombyx*, approximately 20 larvae were collected after just hatching and were fed with fresh mulberry leaves at 25°C for developmental timing.

Generation of transgenic flies

To generate transgenic fly line for *UAS-Hsp70* RNAi, forward and reverse primers with a palindrome structure targeting the exon of the *Hsp70* gene were synthesized by TSINGKE Biological Technology. After annealing the pair of primers, the short double-stranded DNA was subcloned and inserted into the VALIUM20 plasmid. On the basis of the transposable elements in the VALIUM20 plasmid, the DNA fragment was inserted at the attP site in the 25C6 locus on chromosome 2. All related primers used are listed in table S1.

PSG-specific knockout of *USP8* and *Hsp70* in *Bombyx*

On the basis of the binary *Bombyx* PSG-specific CRISPR-Cas9 system we previously established (*7*), gRNA sequences targeting the first exon of the *Bombyx USP8* gene and *Hsp70* gene were designed with the online tool "CRISPR direct" (http://crispr.dbcls.jp/) (*74*). The transgenic *Bombyx* gRNA strains were obtained as we previously reported (*7*). After the PSG-specific *FibH*-Cas9 strains were crossed with *USP8* gRNA and *Hsp70* gRNA transgenic strains separately, the PSGs were dissected for subsequent detection of *Bombyx USP8* and *Hsp70* mutations. After the tissues were ground into very fine powder with liquid nitrogen, the genomic DNA was extracted using phenol/chloroform. The genomic PCR products were extracted using the genomic DNA as a template and specific primers covering the mutation sites in the *USP8* gene and *Hsp70* gene and were then cloned into a T-simple vector for subsequent sequencing. All related primers used are listed in table S1.

Cell culture and ex vivo tissue culture

Drosophila S2 cells and isolated salivary glands were grown in Schneider's *Drosophila* medium (Gibco) supplemented with 10% fetal bovine serum (FBS; Gibco) at 27°C. *Bombyx* BmE cells and isolated PSGs were cultured in Grace's insect cell culture medium supplemented with 10% FBS (Gibco) and 1% penicillin/streptomycin (Gibco) at 27°C.

DNA quantification

The *C* value of the *Drosophila* salivary gland cells was calculated on the basis of the 4′,6-diamidino-2-phenylindole (DAPI) fluorescence intensity as previously described (*25*). Briefly, the salivary glands of wandering *Drosophila* larvae were dissected and stained with DAPI (1:1000; Thermo Fisher Scientific). Z-stack images of individual cell nuclei were then obtained at ×40 magnification (Zeiss LSM 880) under the same laser intensity. The integrated DAPI fluorescence intensity was used for *C* value measurements. The *C* value of a salivary gland cell as the control is set as 1350 C (*75*).

To calculate the *C* value of the *Bombyx* PSG cell, five PSGs from wandering *Bombyx* larvae and 1×10^7 cultured BmE cells were separately collected for genomic DNA extraction. The DNA content was spectrophotometrically quantified using an Agilent 2100 Bioanalyzer System (Agilent) at an optical density of 260 nm. With the 2C genome of diploid BmE cells as a reference, the *C* value of PSG cells was calculated.

Drug treatment

Several inhibitors, including PES (Selleck) that inhibits the interaction between Hsp70 and its partners, VER155008 (Selleck) that inhibits the enzymatic activity of Hsp70, and IN-2 (Selleck) that blocks the enzymatic activity of USP8, were used in the present study. Briefly, for the detection of expression levels or ubiquitination levels, cultured cells and glands were treated with 10 μM PES for 6 hours or treated with 2 μM IN-2 for 12 hours at room temperature. Then, the cells and glands were harvested for Western blotting and RT-qPCR analyses. To detect the effect of Hsp70 on the USP8-Fzr interaction, cells and glands were collected at 2 hours after the treatment with 10 μM PES or 3 μM VER155008, a time point when Fzr protein levels should have no change following the treatment.

EdU incorporation assay

EdU incorporation assay was performed with the commercial Cell Light EdU Apollo 567 Kit (RiboBio) as previously described (*16*). In summary, salivary glands and wing discs were isolated from *Drosophila* larvae 96 hours AEL, and PSGs were isolated on the second day of the fourth larval instar (L4D2), after which the tissues were cultured with EdU (100 μg/ml) in vitro for 2 hours at room temperature according to the manufacturer's protocol. All the tissues were subsequently fixed in 4% formaldehyde for 30 min and then incubated with Apollo dye for 30 min and DAPI for 30 min. After mounting in Vectashield buffer, the fluorescence signals were captured via confocal microscopy (Zeiss LSM 880).

Western blotting

Total protein was isolated from cultured cells and tissues. The protein concentration in each lysate was quantified via the Bradford Method Protein Assay Kit (Sigma-Aldrich) using a microplate reader (BioTek) at an absorbance of 562 nm. Equal amounts of total protein were subjected to Western blotting. The antibodies and dilutions used in the study were as follows: rabbit anti-*Bombyx* Fzr (1:1000; Zoonbio Biotechnology), rabbit anti-*Drosophila* Fzr (1:1000; Zoonbio Biotechnology), rabbit anti-Hsp70 (1:1000; Zoonbio Biotechnology), rabbit anti-USP8 (1:1000; Zoonbio Biotechnology), rabbit anti-*Bombyx* CycB (1:1000; Zoonbio Biotechnology), mouse anti-*Drosophila* CycB (1:1000; Developmental Studies Hybridoma Bank), rabbit anti-CycA (1:1000; Developmental Studies Hybridoma Bank), mouse anti-Flag (1:5000; Sigma-Aldrich), mouse anti-V5 (1:5000; Abcam), mouse anti-HA (1:5000; Abcam), rabbit anti-Ub (1:1000; Proteintech), mouse anti-His (1:5000; Beyotime), mouse anti-GST (1:1000; Beyotime), rabbit anti-luciferase (1:2000; Sigma-Aldrich), and mouse anti-tubulin (1:10,000; Beyotime). The following secondary antibodies were used: horseradish peroxidase–conjugated goat anti-rabbit (1:10,000; Beyotime) and goat anti-mouse (1:10,000; Beyotime).

Immunostaining

An immunostaining assay was performed as previously described (*16*). Briefly, the tissues were fixed with 4% polyformaldehyde for 30 min. The fixed glands were washed three times with PBST buffer [1× phosphate-buffered saline (PBS) containing 0.3% Triton X-100] and then stained at 4°C overnight with the following primary antibodies at the indicated dilutions: rabbit anti-*Bombyx* Fzr (1:50; Zoonbio Biotechnology), rabbit anti-USP8 (1:50; Zoonbio

Biotechnology), rabbit anti-Hsp70 (1:50; Zoonbio Biotechnology), and rabbit anti-pH3 (1:100; Invitrogen). After being washed three times with PBST buffer, the samples were incubated with an Alexa Fluor–conjugated goat anti-rabbit (1:200; Life Technologies) secondary antibody. DAPI (1:1000; Thermo Fisher Scientific) was used for nuclear labeling. Last, after being washed with PBS three times, the tissues were mounted in Vectashield mounting buffer, and the fluorescence signals were captured using a confocal microscope (Zeiss LSM 880).

AlphaFold 3–based modeling of protein interaction

We predicted USP8-Fzr and Hsp70-Fzr interactions using computational tools. Briefly, the projection of protein models was performed using the online AlphaFold 3 (https://alphafoldserver.com/) program and the coupled amino acid sequences of USP8-Fzr and Hsp70-Fzr. Predictions for the docking of USP8-Fzr and Hsp70-Fzr were performed using the HDOCK program with a hybrid docking strategy (*76*, *77*). The results were filtered on the basis of the calculation of the docking scores using ITScorePP to obtain the most reliable docking models (*78*). PyMOL software (version 3.0.3) was used for result analysis and drawing operations.

Co-IP assay

Collected cells or tissues were lysed in NP-40 lysis buffer (Beyotime) containing 1 mM protease inhibitor cocktail (Sigma-Aldrich) on ice for 10 min. After centrifugation at low temperature, the supernatants were collected for subsequent co-IP experiments according to our previously described procedure (*79*). Briefly, the supernatants were incubated with 2 μg of indicated antibodies that were cross-linked with protein G magnetic Dynabeads (Invitrogen) in buffer containing 1 mM protease inhibitor cocktail (Sigma-Aldrich) under gentle rotation at 4°C for 6 hours. Co-IP assay with an anti–immunoglobulin G antibody was set as the control. Then, the antibody-protein complexes were eluted with SDT buffer containing 4% (w/v) SDS and 100 mM tris/HCl (pH 7.4). Last, the eluted samples were subjected to Western blotting analysis.

GST pull-down assay

The open reading frame (ORF) of *Fzr*, *Hsp70*, and *USP8* genes of both *Bombyx* and *Drosophila* were separately subcloned into the pGEX, pCold-SUMO, and pET32M3C vectors. The recombinant vectors were subsequently transformed into the *Escherichia coli* strain BL21, and protein expression was subsequently induced for 20 hours with 0.2 mM isopropyl-β-D-thiogalactopyranoside (Invitrogen) at 16°C to produce the activated GST-Fzr, SUMO-His-Hsp70, and Trx-His-USP8 recombinant proteins. The pGEX, pCold-SUMO, and pET32M3C vectors were used to produce the GST, SUMO-His, and Trx-His proteins, respectively. The GST and GST fusion proteins were purified using glutathione-conjugated agarose beads (Thermo Fisher Scientific). His fusion proteins were purified using nickel-nitrilotriacetic acid (Ni-NTA) agarose beads (Thermo Fisher Scientific).

Glutathione agarose beads (50 μl) coated with either GST or the GST-Fzr recombinant protein (5 mg per sample) were mixed with the His-tagged recombinant proteins (10 mg per sample) separately in 500 μl of PBS (pH 8.0). Each mixture was incubated with shaking for 6 hours at 4°C. The beads were eluted with 200 μl of 50 mM tris-HCl (pH 8.0) containing 10 mM GSH to isolate the supernatant following three washes. Last, the eluted samples were subjected to Western blot analysis.

Reverse transcription quantitative polymerase chain reaction

Total RNA was extracted from glands and cells using TRIzol reagent (Invitrogen), as described previously (*73*). Two micrograms of total RNA was used for template cDNA synthesis with the M-MLV Reverse Transcriptase Kit (Promega). RT-qPCR analyses were performed in triplicate with a NovoStart SYBR qPCR SuperMix (Novoprotein) in a qTower 2.2 Real-time PCR Detection System (Jena). The *Drosophila α-Tubulin at 84B gene* (*α-Tub84B*) and the *Bombyx ribosomal protein L3 gene* (*RpL3*) were used as internal controls. Relative mRNA expression levels were calculated using the 2-ΔΔCT method. All related primers used are listed in table S1.

In vivo protein folding assay

As described previously (*56*–*58*), we performed an in vivo folding assay by assessing the effectiveness of Fzr-luciferase enzyme activity in the context of *Hsp70* overexpression. The ORF sequence of the luciferase-fused Fzr (Fzr-Luc) was subcloned into the *Bombyx* pSL1180 or *Drosophila* pMT-V5-HisA vectors for gene overexpression. At 48 hours after transient cotransfecting of Hsp70 and recombinant Fzr-Luc plasmids into BmE cells or S2 cells, a luciferase assay was performed as described previously (*16*). The total recombinant Fzr-Luc protein levels in the related cells was detected via Western blotting and then was normalized to the tubulin protein levels. The normalized Fzr-Luc protein levels were used as the internal control for luciferase activity analysis.

Protein stability and ubiquitination assays

Protein stability assays were conducted as previously reported (*38*). The cultured cells and glands were treated with CHX (20 μg/ml; Sigma-Aldrich) for the indicated times to inhibit protein synthesis. The proteasome inhibitor MG132 (50 μM; MedChemExpress) and the lysosome inhibitor NH_4Cl (10 mM; Merck) were added to the medium before harvesting. The protein level of Fzr was measured via Western blotting with specific antibodies. For the ubiquitination assays, cells and glands were collected for subsequent immunoprecipitation to obtain ubiquitinated Fzr via the use of a specific anti-Fzr or anti-Flag antibody. The level of ubiquitinated Fzr proteins was subsequently measured via Western blotting with a specific anti-Ub antibody.

ImageJ-based quantitative analysis

Quantitative analysis of the ubiquitin bands in the Western blotting was performed by using the ImageJ software (*79*). First, converted the bands in the IP experiments into Grayscale format and subtracted the background with a value of 50. Second, converted the bands into bright bands and calculated the integrated density of a band by hand drawing an area corresponding to its borders. Third, divided the integrated density value of Ub by the integrated density value of Fzr in the IP experiments and performed normalization analysis.

Statistical analysis

All the data shown in the figures are representative of three independent replicates and are presented as the mean ± SE (error bars). Statistical significance (the *P* value) was evaluated by an unpaired, two-tailed Student's *t* test and is denoted as follows: $*P < 0.05$, $**P < 0.01$, and $***P < 0.001$ versus the control.

Supplementary Materials

This PDF file includes:

Figs. S1 to S21
Table S1

REFERENCES AND NOTES

1. N. Zielke, B. A. Edgar, M. L. DePamphilis, Endoreplication. *Cold Spring Harb. Perspect. Biol.* **5**, a012948 (2013).
2. B. A. Edgar, N. Zielke, C. Gutierrez, Endocycles: A recurrent evolutionary innovation for post-mitotic cell growth. *Nat. Rev. Mol. Cell Biol.* **15**, 197–210 (2014).
3. C. Breuer, T. Ishida, K. Sugimoto, Developmental control of endocycles and cell growth in plants. *Curr. Opin. Plant Biol.* **13**, 654–660 (2010).
4. S. Patra, P. P. Naik, K. K. Mahapatra, M. R. Alotaibi, S. Patil, B. S. Patro, G. Sethi, T. Efferth, S. K. Bhutia, Recent advancement of autophagy in polyploid giant cancer cells and its interconnection with senescence and stemness for therapeutic opportunities. *Cancer Lett.* **590**, 216843 (2024).
5. S. Dhawan, K. P. Gopinathan, Cell cycle events during the development of the silk glands in the mulberry silkworm *Bombyx mori*. *Dev. Genes Evol.* **213**, 435–444 (2003).
6. B. Pino-Jimenez, P. Giannios, J. Casanova, Polyploidy-associated autophagy promotes larval tracheal histolysis at *Drosophila* metamorphosis. *Autophagy.* **19**, 2972–2981 (2023).
7. W. Qian, H. Li, X. Zhang, Y. Tang, D. Yuan, Z. Huang, D. Cheng, Fzr regulates silk gland growth by promoting endoreplication and protein synthesis in the silkworm. *PLOS Genet.* **19**, e1010602 (2023).
8. J. Duan, Y. Zhao, H. Li, L. Habernig, M. D. Gordon, X. Miao, Y. Engstrom, S. Buttner, Bab2 functions as an ecdysone-responsive transcriptional repressor during *Drosophila* development. *Cell Rep.* **32**, 107972 (2020).
9. Y. Ohhara, S. Kobayashi, N. Yamanaka, Nutrient-dependent endocycling in steroidogenic tissue dictates timing of metamorphosis in *Drosophila melanogaster*. *PLOS Genet.* **13**, e1006583 (2017).
10. Y. Ohhara, A. Nakamura, Y. Kato, K. Yamakawa-Kobayashi, Chaperonin TRiC/CCT supports mitotic exit and entry into endocycle in *Drosophila*. *PLOS Genet.* **15**, e1008121 (2019).
11. W. Guo, Z. Wu, J. Song, F. Jiang, Z. Wang, S. Deng, V. K. Walker, S. Zhou, Juvenile hormone-receptor complex acts on *Mcm4* and *Mcm7* to promote polyploidy and vitellogenesis in the migratory locust. *PLOS Genet.* **10**, e1004702 (2014).
12. S. N. Manivannan, J. Roovers, N. Smal, C. T. Myers, D. Turkdogan, F. Roelens, O. Kanca, H. L. Chung, T. Scholz, K. Hermann, T. Bierhals, H. S. Caglayan, H. Stamberger, MAE Working Group of EuroEPINOMICS RES Consortium, H. Mefford, P. de Jonghe, S. Yamamoto, S. Weckhuysen, H. J. Bellen, *De novo FZR1* loss-of-function variants cause developmental and epileptic encephalopathies. *Brain* **145**, 1684–1697 (2022).
13. M. E. Kaplow, A. H. Korayem, T. R. Venkatesh, Regulation of glia number in *Drosophila* by Rap/Fzr, an activator of the anaphase-promoting complex, and Loco, an RGS protein. *Genetics* **178**, 2003–2016 (2008).
14. V. Schaeffer, C. Althauser, H. R. Shcherbata, W. M. Deng, H. Ruohola-Baker, Notch-dependent Fizzy-related/Hec1/Cdh1 expression is required for the mitotic-to-endocycle transition in *Drosophila* follicle cells. *Curr. Biol.* **14**, 630–636 (2004).
15. S. J. Sigrist, C. F. Lehner, *Drosophila* fizzy-related down-regulates mitotic cyclins and is required for cell proliferation arrest and entry into endocycles. *Cell* **90**, 671–681 (1997).
16. W. Qian, Z. Li, W. Song, T. Zhao, W. Wang, J. Peng, L. Wei, Q. Xia, D. Cheng, A novel transcriptional cascade is involved in Fzr-mediated endoreplication. *Nucleic Acids Res.* **48**, 4214–4229 (2020).
17. H. R. Shcherbata, C. Althauser, S. D. Findley, H. Ruohola-Baker, The mitotic-to-endocycle switch in *Drosophila* follicle cells is executed by Notch-dependent regulation of G1/S, G2/M and M/G1 cell-cycle transitions. *Development* **131**, 3169–3181 (2004).
18. L. De Veylder, J. C. Larkin, A. Schnittger, Molecular control and function of endoreplication in development and physiology. *Trends Plant Sci.* **16**, 624–634 (2011).
19. C. Breuer, K. Morohashi, A. Kawamura, N. Takahashi, T. Ishida, M. Umeda, E. Grotewold, K. Sugimoto, Transcriptional repression of the APC/C activator CCS52A1 promotes active termination of cell growth. *EMBO J.* **31**, 4488–4501 (2012).
20. A. Cebolla, J. M. Vinardell, E. Kiss, B. Olah, F. Roudier, A. Kondorosi, E. Kondorosi, The mitotic inhibitor ccs52 is required for endoreduplication and ploidy-dependent cell enlargement in plants. *EMBO J* **18**, 4476–4484 (1999).
21. E. Cohen, N. G. Peterson, J. K. Sawyer, D. T. Fox, Accelerated cell cycles enable organ regeneration under developmental time constraints in the *Drosophila* hindgut. *Dev. Cell* **56**, 2059–2072.e3 (2021).
22. A. C. Pimentel, T. R. Venkatesh, *rap* gene encodes Fizzy-related protein (Fzr) and regulates cell proliferation and pattern formation in the developing *Drosophila* eye-antennal disc. *Dev. Biol.* **285**, 436–446 (2005).
23. K. Narbonne-Reveau, S. Senger, M. Pal, A. Herr, H. E. Richardson, M. Asano, P. Deak, M. A. Lilly, APC/CFzr/Cdh1 promotes cell cycle progression during the *Drosophila* endocycle. *Development* **135**, 1451–1461 (2008).
24. N. Zielke, S. Querings, C. Rottig, C. Lehner, F. Sprenger, The anaphase-promoting complex/cyclosome (APC/C) is required for rereplication control in endoreplication cycles. *Genes Dev.* **22**, 1690–1703 (2008).
25. N. Zielke, K. J. Kim, V. Tran, S. T. Shibutani, M. J. Bravo, S. Nagarajan, M. van Straaten, B. Woods, G. von Dassow, C. Rottig, C. F. Lehner, S. S. Grewal, R. J. Duronio, B. A. Edgar, Control of *Drosophila* endocycles by E2F and CRL4(CDT2). *Nature* **480**, 123–127 (2011).
26. J. W. Raff, K. Jeffers, J. Y. Huang, The roles of Fzy/Cdc20 and Fzr/Cdh1 in regulating the destruction of cyclin B in space and time. *J. Cell Biol.* **157**, 1139–1149 (2002).
27. A. Reber, C. F. Lehner, H. W. Jacobs, Terminal mitoses require negative regulation of Fzr/Cdh1 by Cyclin A, preventing premature degradation of mitotic cyclins and String/Cdc25. *Development* **133**, 3201–3211 (2006).
28. T. Listovsky, Y. S. Oren, Y. Yudkovsky, H. M. Mahbubani, A. M. Weiss, M. Lebendiker, M. Brandeis, Mammalian Cdh1/Fzr mediates its own degradation. *EMBO J.* **23**, 1619–1626 (2004).
29. A. Ciechanover, The unravelling of the ubiquitin system. *Nat. Rev. Mol. Cell Biol.* **16**, 322–324 (2015).
30. T. E. T. Mevissen, D. Komander, Mechanisms of deubiquitinase specificity and regulation. *Annu. Rev. Biochem.* **86**, 159–192 (2017).
31. N. Zheng, N. Shabek, Ubiquitin ligases: Structure, function, and regulation. *Annu. Rev. Biochem.* **86**, 129–157 (2017).
32. K. D. Wilkinson, Ubiquitination and deubiquitination: Targeting of proteins for degradation by the proteasome. *Semin. Cell Dev. Biol.* **11**, 141–148 (2000).
33. F. E. Reyes-Turcu, K. H. Ventii, K. D. Wilkinson, Regulation and cellular roles of ubiquitin-specific deubiquitinating enzymes. *Annu. Rev. Biochem.* **78**, 363–397 (2009).
34. D. Komander, M. Rape, The ubiquitin code. *Annu. Rev. Biochem.* **81**, 203–229 (2012).
35. C. S. Yang, S. A. Sinenko, M. J. Thomenius, A. C. Robeson, C. D. Freel, S. R. Horn, S. Kornbluth, The deubiquitinating enzyme DUBAI stabilizes DIAP1 to suppress *Drosophila* apoptosis. *Cell Death Differ.* **21**, 604–611 (2014).
36. J. Mathieu, P. Michel-Hissier, V. Boucherit, J. R. Huynh, The deubiquitinase USP8 targets ESCRT-III to promote incomplete cell division. *Science* **376**, 818–823 (2022).
37. W. Luo, Y. Li, C. H. Tang, K. C. Abruzzi, J. Rodriguez, S. Pescatore, M. Rosbash, CLOCK deubiquitylation by USP8 inhibits CLK/CYC transcription in *Drosophila*. *Genes Dev.* **26**, 2536–2549 (2012).
38. X. Sun, Y. Ding, M. Zhan, Y. Li, D. Gao, G. Wang, Y. Gao, Y. Li, S. Wu, L. Lu, Q. Liu, Z. Zhou, Usp7 regulates Hippo pathway through deubiquitinating the transcriptional coactivator Yorkie. *Nat. Commun.* **10**, 411 (2019).
39. Z. Zhou, X. Yao, S. Li, Y. Xiong, X. Dong, Y. Zhao, J. Jiang, Q. Zhang, Deubiquitination of Ci/Gli by Usp7/HAUSP regulates Hedgehog signaling. *Dev. Cell.* **34**, 58–72 (2015).
40. B. F. Costantino, D. K. Bricker, K. Alexandre, K. Shen, J. R. Merriam, C. Antoniewski, J. L. Callender, V. C. Henrich, A. Presente, A. J. Andres, A novel ecdysone receptor mediates steroid-regulated developmental events during the mid-third instar of *Drosophila*. *PLOS Genet.* **4**, e1000102 (2008).
41. Z. Li, W. Qian, W. Song, T. Zhao, Y. Yang, W. Wang, L. Wei, D. Zhao, Y. Li, N. Perrimon, Q. Xia, D. Cheng, A salivary gland-secreted peptide regulates insect systemic growth. *Cell Rep.* **38**, 110397 (2022).
42. S. B. Pierce, C. Yost, J. S. Britton, L. W. Loo, E. M. Flynn, B. A. Edgar, R. N. Eisenman, dMyc is required for larval growth and endoreplication in *Drosophila*. *Development* **131**, 2317–2327 (2004).
43. J. Z. Maines, L. M. Stevens, X. Tong, D. Stein, *Drosophila* dMyc is required for ovary cell growth and endoreplication. *Development* **131**, 775–786 (2004).
44. A. Hershko, A. Ciechanover, The ubiquitin system. *Annu. Rev. Biochem.* **67**, 425–479 (1998).
45. A. Ciechanover, Proteolysis: From the lysosome to ubiquitin and the proteasome. *Nat. Rev. Mol. Cell Biol.* **6**, 79–87 (2005).
46. J. Abramson, J. Adler, J. Dunger, R. Evans, T. Green, A. Pritzel, O. Ronneberger, L. Willmore, A. J. Ballard, J. Bambrick, S. W. Bodenstein, D. A. Evans, C. C. Hung, M. O'Neill, D. Reiman, K. Tunyasuvunakool, Z. Wu, A. Zemgulyte, E. Arvaniti, C. Beattie, O. Bertolli, A. Bridgland, A. Cherepanov, M. Congreve, A. I. Cowen-Rivers, A. Cowie, M. Figurnov, F. B. Fuchs, H. Gladman, R. Jain, Y. A. Khan, C. M. R. Low, K. Perlin, A. Potapenko, P. Savy, S. Singh, A. Stecula, A. Thillaisundaram, C. Tong, S. Yakneen, E. D. Zhong, M. Zielinski, A. Zidek, V. Bapst, P. Kohli, M. Jaderberg, D. Hassabis, J. M. Jumper, Accurate structure prediction of biomolecular interactions with AlphaFold 3. *Nature* **630**, 493–500 (2024).
47. Y. Zhao, D. Peng, Y. Liu, Q. Zhang, B. Liu, Y. Deng, W. Ding, Z. Zhou, Q. Liu, Usp8 promotes tumor cell migration through activating the JNK pathway. *Cell Death Dis.* **13**, 286 (2022).
48. R. Rosenzweig, N. B. Nillegoda, M. P. Mayer, B. Bukau, The Hsp70 chaperone network. *Nat. Rev. Mol. Cell Biol.* **20**, 665–680 (2019).
49. M. P. Mayer, B. Bukau, Hsp70 chaperones: Cellular functions and molecular mechanism. *Cell. Mol. Life Sci.* **62**, 670–684 (2005).
50. F. U. Hartl, A. Bracher, M. Hayer-Hartl, Molecular chaperones in protein folding and proteostasis. *Nature* **475**, 324–332 (2011).
51. M. P. Mayer, Hsp70 chaperone dynamics and molecular mechanism. *Trends Biochem. Sci.* **38**, 507–514 (2013).

52. J. I.-J. Leu, J. Pimkina, A. Frank, M. E. Murphy, D. L. George, A small molecule inhibitor of inducible heat shock protein 70. *Mol. Cell* **36**, 15–27 (2009).
53. H. H. Kampinga, E. A. Craig, The HSP70 chaperone machinery: J proteins as drivers of functional specificity. *Nat. Rev. Mol. Cell Biol.* **11**, 579–592 (2010).
54. C. M. Dobson, Protein folding and misfolding. *Nature* **426**, 884–890 (2003).
55. R. Fraschini, A. Beretta, L. Sironi, A. Musacchio, G. Lucchini, S. Piatti, Bub3 interaction with Mad2, Mad3 and Cdc20 is mediated by WD40 repeats and does not require intact kinetochores. *EMBO J.* **20**, 6648–6659 (2001).
56. J.-Y. Cha, J. Kim, T.-S. Kim, Q. Zeng, L. Wang, S. Y. Lee, W.-Y. Kim, D. E. Somers, GIGANTEA is a co-chaperone which facilitates maturation of ZEITLUPE in the *Arabidopsis* circadian clock. *Nat. Commun.* **8**, 3 (2017).
57. B. C. Freeman, A. Michels, J. Song, H. H. Kampinga, R. I. Morimoto, Analysis of molecular chaperone activities using in vitro and in vivo approaches. *Methods Mol. Biol.* **99**, 393–419 (2000).
58. A. Bepperling, F. Alte, T. Kriehuber, N. Braun, S. Weinkauf, M. Groll, M. Haslbeck, J. Buchner, Alternative bacterial two-component small heat shock protein systems. *Proc. Natl. Acad. Sci. U.S.A.* **109**, 20407–20412 (2012).
59. L. Rinaldi, R. Delle Donne, B. Catalanotti, O. Torres-Quesada, F. Enzler, F. Moraca, R. Nistico, F. Chiuso, S. Piccinin, V. Bachmann, H. H. Lindner, C. Garbi, A. Scorziello, N. A. Russo, M. Synofzik, U. Stelzl, L. Annunziato, E. Stefan, A. Feliciello, Feedback inhibition of cAMP effector signaling by a chaperone-assisted ubiquitin system. *Nat. Commun.* **10**, 2572 (2019).
60. F. Meghini, T. Martins, X. Tait, K. Fujimitsu, H. Yamano, D. M. Glover, Y. Kimata, Targeting of Fzr/Cdh1 for timely activation of the APC/C at the centrosome during mitotic exit. *Nat. Commun.* **7**, 12607 (2016).
61. J. A. Pesin, T. L. Orr-Weaver, Regulation of APC/C activators in mitosis and meiosis. *Annu. Rev. Cell Dev. Biol.* **24**, 475–499 (2008).
62. A. Zur, M. Brandeis, Timing of APC/C substrate degradation is determined by fzy/fzr specificity of destruction boxes. *EMBO J.* **21**, 4500–4510 (2002).
63. H. Jacobs, D. Richter, T. Venkatesh, C. Lehner, Completion of mitosis requires neither fzr/rap nor fzr2, a male germline-specific *Drosophila* Cdh1 homolog. *Curr. Biol.* **12**, 1435–1441 (2002).
64. R. J. Duronio, P. H. O'Farrell, Developmental control of the G1 to S transition in *Drosophila*: Cyclin E is a limiting downstream target of E2F. *Genes Dev.* **9**, 1456–1468 (1995).
65. J. Sun, W. M. Deng, Notch-dependent downregulation of the homeodomain gene *cut* is required for the mitotic cycle/endocycle switch and cell differentiation in *Drosophila* follicle cells. *Development* **132**, 4299–4308 (2005).
66. H. Lopez-Schier, D. St Johnston, Delta signaling from the germ line controls the proliferation and differentiation of the somatic follicle cells during *Drosophila* oogenesis. *Genes Dev.* **15**, 1393–1405 (2001).
67. J. Zeng, N. Huynh, B. Phelps, K. King-Jones, Snail synchronizes endocycling in a TOR-dependent manner to coordinate entry and escape from endoreplication pausing during the *Drosophila* critical weight checkpoint. *PLOS Biol.* **18**, e3000609 (2020).
68. Z. Wu, W. Guo, L. Yang, Q. He, S. Zhou, Juvenile hormone promotes locust fat body cell polyploidization and vitellogenesis by activating the transcription of *Cdk6* and *E2f1*. *Insect Biochem. Mol. Biol.* **102**, 1–10 (2018).
69. D. S. Latchman, Heat shock proteins and cardiac protection. *Cardiovasc. Res.* **51**, 637–646 (2001).
70. H. Gao, X. Yuan, J. Wang, Y. Yan, X. Zhang, T. He, X. Lin, H. Zhang, Z. Liu, Knockdown of *Fzr* inhibited the growth of *Nilaparvata lugens* by blocking endocycle. *Pest Manag. Sci.* **81**, 36–43 (2025).
71. I. Garcia-Higuera, E. Manchado, P. Dubus, M. Canamero, J. Mendez, S. Moreno, M. Malumbres, Genomic stability and tumour suppression by the APC/C cofactor Cdh1. *Nat. Cell Biol.* **10**, 802–811 (2008).
72. W. Qian, M. Guo, J. Peng, T. Zhao, Z. Li, Y. Yang, H. Li, X. Zhang, K. King-Jones, D. Cheng, Decapentaplegic retards lipolysis during metamorphosis in *Bombyx mori* and *Drosophila melanogaster*. *Insect Biochem. Mol. Biol.* **155**, 103928 (2023).
73. Y. Yang, T. Zhao, Z. Li, W. Qian, J. Peng, L. Wei, D. Yuan, Y. Li, Q. Xia, D. Cheng, Histone H3K27 methylation–mediated repression of *Hairy* regulates insect developmental transition by modulating ecdysone biosynthesis. *Proc. Natl. Acad. Sci. U.S.A.* **118**, e2101442118 (2021).
74. Y. Naito, K. Hino, H. Bono, K. Ui-Tei, CRISPRdirect: Software for designing CRISPR/Cas guide RNA with reduced off-target sites. *Bioinformatics* **31**, 1120–1123 (2015).
75. M. P. Hammond, C. D. Laird, Control of DNA replication and spatial distribution of defined DNA sequences in salivary gland cells of *Drosophila melanogaster*. *Chromosoma* **91**, 279–286 (1985).
76. Y. Yan, H. Tao, J. He, S. Y. Huang, The HDOCK server for integrated protein-protein docking. *Nat. Protoc.* **15**, 1829–1852 (2020).
77. Y. Yan, Z. Wen, X. Wang, S. Y. Huang, Addressing recent docking challenges: A hybrid strategy to integrate template-based and free protein-protein docking. *Proteins* **85**, 497–512 (2017).
78. S. Y. Huang, X. Zou, A knowledge-based scoring function for protein-RNA interactions derived from a statistical mechanics-based iterative method. *Nucleic Acids Res.* **42**, e55 (2014).
79. W. Qian, X. Gang, T. Zhang, L. Wei, X. Yang, Z. Li, Y. Yang, L. Song, P. Wang, J. Peng, D. Cheng, Q. Xia, Protein kinase A-mediated phosphorylation of the Broad-Complex transcription factor in silkworm suppresses its transcriptional activity. *J. Biol. Chem.* **292**, 12460–12470 (2017).

Acknowledgments: We thank the TsingHua Fly Center, Vienna *Drosophila* Resource Center, National Institute of Genetics at Japan, Bloomington *Drosophila* Stock Center, and FlyORF for providing the fly lines. **Funding:** This work was supported by National Natural Science Foundation of China 32200404 (W.Q.), National Natural Science Foundation of China 32370555 (D.C.), Technology Innovation and Application Development Program of Chongqing CSTB2024TIAD-KPX0023 (D.C.), National Natural Science Foundation of China 32070496 (D.C.), National Natural Science Foundation of China 31772679 (D.C.), and Natural Science Foundation of Chongqing 2024NSCQ-qncxX0192 (W.Q.). **Author contributions:** Conceptualization: D.C. and W.Q. Methodology: D.C. and W.Q. Project administration: D.C. Investigation: W.Q., X.Z., D.Y., Y.W., H.L., Z.L., Z.D., P.S., and Q.S. Visualization: D.C., W.Q., X.Z., D.Y., and L.W. Validation: D.C., W.Q., X.Z., D.Y., Y.W., H.L., Z.L., Z.D., P.S., and Q.S. Resources: X.Z., D.Y., L.W., and Z.Z., Software: X.Z. and D.Y. Formal analysis: D.C., W.Q., X.Z., D.Y., and Q.X. Supervision: D.C. Data curation: W.Q. Funding acquisition: D.C. and W.Q. Writing—original draft: D.C., W.Q., X.Z., and D.Y. Writing—review and editing: D.C., W.Q., X.Z., and D.Y. **Competing interests:** The authors declare that they have no competing interests. **Data and materials availability:** All data needed to evaluate the conclusions in the paper are present in the paper and/or the Supplementary Materials.

Submitted 5 June 2024
Accepted 11 February 2025
Published 19 March 2025
10.1126/sciadv.adq9111